

How to Combine Differential Privacy and Continual Learning

Marlon Tobaben^{*1} Talal Alrawajfeh^{*1} Marcus Klasson² Mikko Heikkilä¹ Arno Solin² Antti Honkela¹

Abstract

The goal of continual learning (CL) is to retain knowledge across tasks, but this conflicts with strict privacy required for sensitive training data that prevents storing or memorising individual samples. This work explores the intersection of CL and differential privacy (DP). We advance the theoretical understanding and introduce methods for combining CL and DP. We formulate and clarify the theory for DP CL focusing on composition over tasks. We introduce different variants of choosing classifiers' output label space, show that choosing the output label space directly based on the task data is not DP, and offer a DP alternative. We propose a method for combining pre-trained models with DP prototype classifiers and parameter-efficient adapters learned under DP to address the trade-offs between privacy and utility in a CL setting. We also demonstrate the effectiveness of our methods for varying degrees of domain shift, for blurry tasks, and with different output label settings.

1. Introduction

Continual learning (CL, McCloskey & Cohen 1989; De Lange et al. 2021; Wang et al. 2024) develops models that learn from a stream of tasks while retaining previous knowledge, a key requirement for real-world applications where data arrives sequentially. However, CL faces the challenge of catastrophic forgetting, where the model loses performance on earlier tasks as it learns new ones (French, 1999). While CL therefore fights for memorising prototypical aspects of the data to prevent catastrophic forgetting, often utilising a memory buffer to store some individual representative samples (Lopez-Paz & Ranzato, 2017), this violates strict privacy requirements necessary for handling sensitive training data.

¹Department of Computer Science, University of Helsinki, Finland ²Department of Computer Science, Aalto University, Finland. Correspondence to: Arno Solin <arno.solin@aalto.fi>, Antti Honkela <antti.honkela@helsinki.fi>.

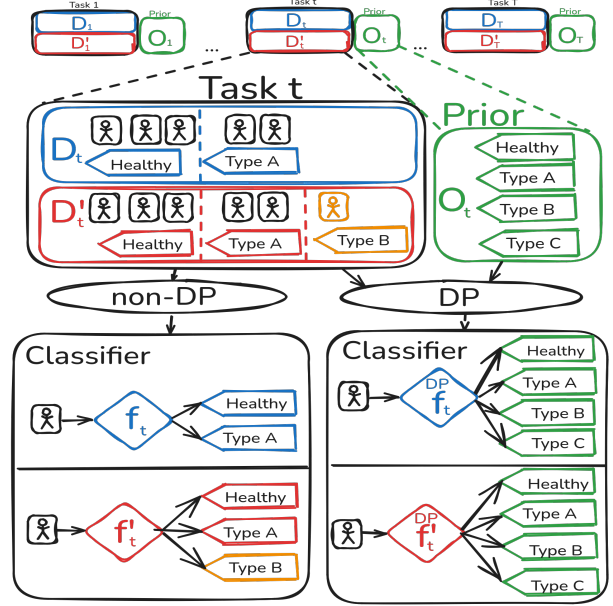


Figure 1. The CL setting consists of T tasks each having a dataset which could be either D_t or the adjacent D'_t (one more datapoint \otimes). The non-DP classifiers f_t/f'_t leak whether D_t or D'_t was used because f'_t outputs one more label \triangleleft than f_t as \otimes is the only datapoint with that label \triangleleft . The DP classifiers' labels \triangleleft are based on prior public knowledge O_t^{prior} resulting in no leakage.

In turn, differential privacy (DP, Dwork et al. 2006b) is a formal privacy definition, which prevents the memorisation of any individual's data in the first place: under DP, the inclusion or exclusion of any single data point does not significantly impact the outcome of the learning process. DP enables machine learning (ML) models to, *e.g.*, comply with privacy regulations (such as GDPR) while being more robust to various privacy attacks (Shokri et al., 2017; Balle et al., 2022; Haim et al., 2022). In other words, instead of memorising sensitive individual data, DP enforces algorithms to provably generalise beyond the specific samples seen in training (Jung et al., 2021). While DP is crucial for privacy-preserving ML, it also introduces an unavoidable trade-off: stronger privacy often degrades model utility (Ponomareva et al., 2023).

In this work, we combine DP with CL. This presents unique challenges both to satisfy the demands of mitigating catastrophic forgetting without violating privacy, as well as to

minimise the negative effect privacy has on model utility. We first formally define differentially private continual learning (DP CL) as task-wise DP, relate it to prior work (Chen et al., 2022; Desai et al., 2021; Farquhar & Gal, 2019; Hassanpour et al., 2022; Lai et al., 2022), and clarify the existing theory, especially on composing privacy over multiple tasks. We also highlight a potential issue with DP CL model label output spaces overlooked in existing work, which can lead to catastrophic privacy leakage, and propose sufficient assumptions to address the problem.

Improving the utility using pre-trained models has been recently studied under DP (Kurakin et al., 2022; De et al., 2022; Tobaben et al., 2023), and separately in CL (Janson et al., 2022; Wang et al., 2022a;b). To the best of our knowledge, there is no prior work exploring whether pre-training can ease the tension between privacy and performance over time. We therefore propose two methods utilising pre-trained models that enable CL of new tasks under DP constraints with improved utility. Our algorithms build on successful approaches in non-private CL using pre-trained models: (i) prototype-based classifiers (Janson et al., 2022), and (ii) parameter-efficient adapters (Gao et al., 2023). We extensively demonstrate the effectiveness of our methods in the class-incremental setting (van de Ven et al., 2022), where the goal is to continuously learn a classifier that can discriminate a growing number of classes.

Our contributions can be summarised as follows:

1. **DP CL formalisation:** We formulate and clarify the theory for task-wise DP CL focusing especially on composition over tasks (Sec. 4).
2. **DP CL classification output label space:** We introduce different variants of choosing the classification output label space (Sec. 4.2), show that classifiers can leak information of sensitive data when the output label space directly depends on the data (Sec. 4.3), and offer a DP alternative (Sec. 4.4) by leveraging data-independent prior information.
3. **DP CL methods with pre-trained models:** We propose two DP CL methods for classification with pre-trained models (i) Cosine Classifier (Sec. 5.1), and (ii) Parameter-Efficient Fine-Tuning (PEFT) Ensemble (Sec. 5.2).
4. **Experimental results:** We show that our methods balance privacy and catastrophic forgetting, as well as utility (predictive accuracy), for (i) varying degrees of domain shift between tasks and pre-training data and between different tasks (Sec. 6.1), (ii) blurry tasks (Sec. 6.2), and (iii) different output label settings (Sec. 6.3).

2. Related Work

Differential Privacy In terms of privacy-preserving ML, DP (Dwork et al., 2006b) provides provable privacy guaran-

tees, where the DP-SGD algorithm (Rajkumar & Agarwal, 2012; Song et al., 2013; Abadi et al., 2016) is the standard learning approach. The main challenge is the trade-off between privacy and utility, *i.e.*, how to achieve the similar model behaviours and performance as a non-private model without memorising individual data records. Ensuring privacy in deep learning models has recently gained great interest (Xu et al., 2023; Pelikan et al., 2023) due to their high utility on large-scale data sets. The usage of pre-trained models has increased in popularity (Kurakin et al., 2022; De et al., 2022; Mehta et al., 2023; Cattani et al., 2022; Li et al., 2022; Yu et al., 2022; Tobaben et al., 2023; Tito et al., 2023; Wahdany et al., 2024) with most state-of-the-art models relying on the assumption that the pre-training data is public. However, following the discussion of Tramèr et al. (2024), we utilise pre-trained models trained on pre-training data that is small enough in size as carefully curating large pre-training data sets is very resource intensive/expensive (Thiel, 2023). If private information is contained in the pre-trained data, the DP privacy guarantees in regard to the fine-tuning data become meaningless.

Continual Learning Approaches to mitigate catastrophic forgetting have involved replaying stored examples (Chaudhry et al., 2019), using regularisation techniques (Li & Hoiem, 2017), and expanding networks (Yoon et al., 2018). Recently, to facilitate generalisation to new tasks, pre-trained models in CL settings have been combined with replay (Ostapenko et al., 2022), prompt tuning (Wang et al., 2022a;b), prototype classifiers (Janson et al., 2022; McDonnell et al., 2023), and expandable PEFT adapters (Zhao et al., 2024b; Zhou et al., 2024b;a). We propose DP-variants of prototype classifiers and expandable adapters with pre-trained models to enhance the utility and mitigate forgetting while fulfilling the privacy budget. We experiment in the standard class-incremental learning setting (van de Ven et al., 2022) without task labels and in blurry task boundary settings (Aljundi et al., 2019; Koh et al., 2022; Moon et al., 2023).

Differentially Private Continual Learning Previous works combining DP with CL have leveraged DP synthetic samples or episodic memories (Lopez-Paz & Ranzato, 2017). Farquhar & Gal (2019) train a generative model under DP, while Chen et al. (2022) learn a small set of synthetic samples optimised towards the downstream task. However, these methods have only demonstrated results on MNIST or CIFAR-10, possibly since generating DP-synthetic images of larger resolutions is challenging (Ghalebikesabi et al., 2023). Desai et al. (2021); Lai et al. (2022); Hassanpour et al. (2022) use episodic memories to mitigate catastrophic forgetting, which may violate privacy regulations where previous data is prohibited to store or can only be stored for a certain period of time. On the theoretic end, Lai et al. (2022) introduce a formal definition for life-

long DP and propose lifelong neighboring databases which makes the data adjacency relation local, *i.e.* to each task, instead of being defined globally over all tasks. However, in App. B, we argue that their definition of ϵ -Lifelong learning is limited to parallel composition.

In this paper, we define task-wise DP which is a general definition of computing privacy bounds for independently for each task. Furthermore, we show that a classifier can leak information about sensitive data via its output label space when the label space depends directly on the data as in the CL setting. To this end, we propose a DP alternative where we assume which classes the classifier should learn in the CL tasks is given as prior knowledge. Although this assumption is a restriction in the standard CL setting, we are the first to highlight this limitation of applying DP in CL and suggest how these should be combined to the best of our knowledge.

3. Background

Continual Learning Setting We focus on the continual learning of classification tasks, where we let a model f_θ parameterised by θ learn T tasks sequentially from the data sets $\mathcal{D}_1, \dots, \mathcal{D}_T$. The t^{th} data set $\mathcal{D}_t = \{(x_t^{(i)}, y_t^{(i)})\}_{i=1}^{N_t}$ consists of N_t samples where $x_t^{(i)} \in \mathbb{R}^m$ and $y_t^{(i)} \in \mathbb{N}$ are the i -th data point and class label respectively. Note that the previous data sets are inaccessible in the succeeding tasks. Recently, using pre-trained models as f_θ^{pre} has gained interest in CL where the task classifiers can be (i) linear layers learned via the cross-entropy loss for new tasks (Wang et al., 2022b), or (ii) based on prototypes computed from feature vectors (Janson et al., 2022).

Differential Privacy Formally, we define DP as follows.

Definition 3.1 (DP, Dwork et al. 2006b;a). A randomized algorithm \mathcal{A} is (ϵ, δ) -DP, if for any two neighboring datasets, denoted $\mathcal{D} \simeq \mathcal{D}'$, and for any outcome $S \subseteq \text{Range}(\mathcal{A})$,

$$\Pr[\mathcal{A}(\mathcal{D}) \in S] \leq \exp(\epsilon) \times \Pr[\mathcal{A}(\mathcal{D}') \in S] + \delta, \quad (1)$$

where $\text{Range}(\mathcal{A})$ is the set of all possible outcomes of \mathcal{A} .

The privacy parameters $\epsilon > 0$ and $\delta \in [0, 1]$ in Definition 3.1 control the allowed privacy loss (smaller values mean better privacy). Depending on the chosen neighborhood definition, the granularity of the privacy protection can be tuned. A very common setting is sample-level DP with add/remove neighbors, which we also use in this paper:

Definition 3.2 (Sample-level adjacency). Two datasets \mathcal{D} and \mathcal{D}' are said to be adjacent (or neighbors, written $\mathcal{D} \simeq \mathcal{D}'$) if they differ at most by the addition or removal of a single sample $\|\mathcal{D} - \mathcal{D}'\|_1 = |(\mathcal{D} \setminus \mathcal{D}') \cup (\mathcal{D}' \setminus \mathcal{D})| = 1$.

In deep learning, the algorithm \mathcal{A} can be, *e.g.*, a DP optimisation method which produces a parameter set θ , or a

method for computing class-specific features for producing DP prototypes. The common optimisation approach uses DP-SGD, which minimises an empirical loss while clipping and adding noise to the per-sample gradients to guarantee DP (see Song et al. 2013; Abadi et al. 2016; Ponomareva et al. 2023 for details). In this case, every access to the sensitive data during training, *i.e.*, every gradient calculation, accumulates privacy loss; in other words, the privacy properties of running multiple DP algorithms or one DP algorithm several times compose over the repetitions. Calculating the total privacy over compositions is usually called privacy accounting (Koskela et al., 2020; Gopi et al., 2021).

4. Formalizing DP CL for Classification

Integrating DP into CL for classification when each task introduces new labels is challenging. Some of the existing works on DP CL, including Desai et al. (2021) and Lai et al. (2022), introduce a definition for DP with CL along with a dataset adjacency relation (see App. B for the full discussion); however, these works have several limitations:

1. **Dataset adjacency relation (Sec. 4.1):** Prior DP CL work (Desai et al., 2021; Hassanpour et al., 2022) bases the dataset adjacency, that is required for the privacy accounting for a task t , on assumptions about the future tasks $t + 1, \dots, \infty$. Lai et al. (2022), on the other hand, define the dataset adjacency for each task separately but their approach is limited only to parallel composition. We define task-wise DP in Sec. 4.1 which is a way of computing the privacy bounds for a task t independent of assumptions or knowledge regarding other tasks, and is not restricted to parallel composition.
2. **Target label space (Sec. 4.2):** Classification tasks require careful choice of the target label space. A classifier can leak information about the sensitive data through the output label space if the label space depends directly on the data, as we formally show in Sec. 4.3. We offer a DP alternative in Sec. 4.4. As far as we know, this issue has not been addressed by any prior work on DP CL.
3. **Episodic memory:** Some prior work on DP CL utilize episodic memory which stores individual samples for later use (Desai et al., 2021; Lai et al., 2022). In the sensitive data setting that we consider, storing data for any extended period of time, *i.e.*, over the task boundaries, should be avoided. We do not store any samples.

4.1. Task-Wise DP

To guarantee privacy in CL, our basic approach is to define (sample-level) task-wise DP, given in Definition 4.1, to provide provable privacy for each separate task. Composition methods (McSherry, 2010; Dwork et al., 2010b; Whitehouse et al., 2023) are then applied to account for the privacy over the required number of tasks.

Definition 4.1 (Task-wise DP). Any sequence of independent mechanisms $(\mathcal{M}_t)_{t \in I}$, where $I \subseteq \mathbb{N}$ is a set of task indices that can be either finite or infinite, is said to satisfy task-wise (ϵ, δ) -DP if for all $t \in I$, all adjacent datasets $\mathcal{D}_t \simeq \mathcal{D}'_t$, and all sets $S_t \subseteq \text{Range}(\mathcal{M}_t)$:

$$\Pr[\mathcal{M}_t(\mathcal{D}_t) \in S_t] \leq \exp(\epsilon) \times \Pr[\mathcal{M}_t(\mathcal{D}'_t) \in S_t] + \delta. \quad (2)$$

Task-wise DP means that the neighboring datasets are task-specific, *i.e.* that for any t , we consider datasets $\mathcal{D}_t \simeq \mathcal{D}'_t$ in Definitions 3.1 and 3.2. This contrasts with some previous works, such as Desai et al. (2021); Hassanpour et al. (2022), who define neighbors based on data from all tasks.

Parallel composition (McSherry, 2010) is achieved by splitting the dataset into disjoint subsets, where each privacy unit appears once in only one of the subsets, and running a DP mechanism on each of these subsets separately. The parallel composition is (ϵ, δ) -DP if each DP mechanism is (ϵ, δ) -DP. On the other hand, sequential composition causes a decrease in the privacy level each time we compose. Adaptive sequential composition (Dwork & Roth, 2014; Dwork et al., 2010b) can be used when the privacy parameters, including the number of compositions (*i.e.*, tasks), are known beforehand; otherwise, fully adaptive composition is needed (Whitehouse et al., 2023).

Practically, to achieve task-wise DP, we train and release a DP classifier in each task $t \in I$ on a dataset \mathcal{D}_t using any available DP method. Denote the set of privacy units in dataset \mathcal{D}_t as $\text{units}(\mathcal{D}_t)$. These are the units of privacy that we want to protect which can be the \mathbf{x} s or more coarser components which different \mathbf{x} s can be part of. We can write this classifier as $f_{\theta_t} : \mathcal{X} \rightarrow \mathcal{O}_t$, where θ_t denotes the weights, \mathcal{X} is the input space with $\mathcal{X}_t \subseteq \mathcal{X}$ for all t , and \mathcal{O}_t contains the set of labels for the classifier. The (output) label space for the classifier f_{θ_t} has a unique symbol, *i.e.* \mathcal{O}_t , to enable the study of variants of the label space. We discuss these variants in Sec. 4.2. The mechanism that releases the classifiers for each task is introduced in the following definition.

Definition 4.2 (Classifier-release mechanism). For any t and any dataset \mathcal{D}_t , the randomized mechanism that releases a classifier at tasks t is given by:

$$\mathcal{M}_t : (\mathcal{D}_t) \mapsto (f_{\theta_t} : \mathcal{X} \rightarrow \mathcal{O}_t). \quad (3)$$

We will write f_t to denote the function $f_{\theta_t} : \mathcal{X} \rightarrow \mathcal{O}_t$.

If the sequence of classifier-release mechanisms $(\mathcal{M}_t)_{t \in I}$ is task-wise (ϵ, δ) -DP, we want to define their composition and compute its privacy guarantees:

$$\mathcal{M} : \underbrace{(\mathcal{D}_t)_{t \in I}}_{\text{private}} \mapsto \underbrace{(\mathcal{M}_t(\mathcal{D}_t))_{t \in I}}_{\text{public}}. \quad (4)$$

Lemma 4.3. If $(\mathcal{M}_t)_{t \in I}$ is task-wise (ϵ, δ) -DP, then \mathcal{M}_t is (ϵ, δ) -DP for all $t \in I$.

The proof of Lemma 4.3 can be found in App. C.1. This lemma enables us to translate the task-wise DP guarantees to DP guarantees for each task separately.

Theorem 4.4 (Parallel composition). If $(\mathcal{M}_t)_{t \in I}$ is task-wise (ϵ, δ) -DP, and $\text{units}(\mathcal{D}_i) \cap \text{units}(\mathcal{D}_j) = \emptyset$ for all $i \neq j$, then their composition in Eq. (4) is (ϵ, δ) -DP.

The proof of Theorem 4.4 can be found in App. C.2. The theorem states that if the privacy units are disjoint between subsets, then \mathcal{M} is the parallel composition of the task-wise mechanisms.

Theorem 4.5 (Sequential composition). If $(\mathcal{M}_t)_{t \in I}$ is task-wise (ϵ, δ) -DP, then their composition in Eq. (4) can be written as the sequential composition of $|I|$ (ϵ, δ) -DP mechanisms.

The proof of Theorem 4.5 can be found in App. C.3. When the privacy units between datasets are not disjoint, then both adaptive and fully adaptive composition can be applied to obtain privacy guarantees for \mathcal{M} . The detailed discussion and full theoretical results regarding the composition under task-wise DP can be found in App. C.

4.2. Variants of Choosing Classifier Output Space \mathcal{O}_t

If a classifier $f_t = f_{\theta_t} : \mathcal{X} \rightarrow \mathcal{O}_t$ is released with DP weights θ_t , the mechanism that trains and releases this classifier might still not be DP, depending on the choice of \mathcal{O}_t (output label space). One way to set \mathcal{O}_t is by taking the labels from the task datasets \mathcal{D}_t , *i.e.* setting $\mathcal{O}_t := \mathcal{O}_t^{\text{data}} = \{y : (\mathbf{x}, y) \in \mathcal{D}_t\}$. To help understanding, we imagine there are two parties: i) a *trusted data aggregator*, who has access to the sensitive data \mathcal{D}_t , responsible for training each classifier f_t under DP for any t , and ii) an *adversary*, who has full access to each classifier f_t , including to the weights θ_t and to the label set \mathcal{O}_t , after training. Note that these parties are not necessary for the theory to hold, and the theory could be also applied when the data is stored among multiple parties.

Not directly using $\mathcal{O}_t^{\text{data}}$ may seem restrictive at first; however, we mitigate this by introducing a set of public labels $\mathcal{O}_t^{\text{prior}}$. The set $\mathcal{O}_t^{\text{prior}}$ is assumed to be known to the adversary and represents public or general prior knowledge about the classes in a given task t . On the other hand, $\mathcal{O}_t^{\text{data}}$ is only known by the trusted aggregator. The adversary might expect the dataset to include some classes, but the actual set $\mathcal{O}_t^{\text{prior}}$ might have more, less, or even (partially) different classes. However, we show that the use of publicly known labels is required to guarantee DP (Sec. 4.3). In practice, this is important, especially in our CL experiments, because the individual tasks have relatively small datasets and new

Table 1. A classifier’s output label space \mathcal{O}_t can be either inferred from the sensitive data directly $\langle \square \rangle$ or based on public prior knowledge on what labels could be included in the tasks $\langle \square \rangle$. Only $\langle \square \rangle$ is non-sensitive information, but it might not exactly match the labels of the sensitive data $\langle \square \rangle$. We consider three possible settings to choose \mathcal{O}_t : (i) \mathbf{S}_{data} : \mathcal{O}_t is inferred from classes in sensitive data (not DP, see Sec. 4.3). (ii) $\mathbf{S}_{\text{prior}}$: \mathcal{O}_t is based on task-wise prior knowledge, i.e., what classes are to be expected in a specific task t (iii) $\mathbf{S}_{\text{prior}}^{\text{const}}$: \mathcal{O}_t is based on constant prior knowledge that is not specific to tasks.

		Task 1	Task 2	Task 3	Public	DP
Source of labels	$\mathcal{O}_t^{\text{data}}$ (Sensitive data)	$\langle o_1 \rangle \langle o_2 \rangle$	$\langle o_1 \rangle \langle o_4 \rangle \langle o_5 \rangle$	$\langle o_4 \rangle \langle o_6 \rangle$	✗	-
	$\mathcal{O}_t^{\text{prior}}$ (Task-wise prior public knowledge)	$\langle o_1 \rangle \langle o_2 \rangle \langle o_3 \rangle$	$\langle o_3 \rangle \langle o_4 \rangle$	$\langle o_4 \rangle \langle o_6 \rangle$	✓	-
	$\mathcal{O}^{\text{prior}}$ (Constant prior public knowledge)	$\langle o_1 \rangle \langle o_2 \rangle \langle o_3 \rangle$	$\langle o_2 \rangle \langle o_3 \rangle \langle o_4 \rangle$	$\langle o_6 \rangle$	✓	-
How classifier output space \mathcal{O}_t is determined	\mathbf{S}_{data} (From sensitive data)	$\langle o_1 \rangle \langle o_2 \rangle$	$\langle o_1 \rangle \langle o_4 \rangle \langle o_5 \rangle$	$\langle o_4 \rangle \langle o_6 \rangle$	-	✗
	$\mathbf{S}_{\text{prior}}$ (From task-wise prior knowledge)	$\langle o_1 \rangle \langle o_2 \rangle \langle o_3 \rangle$	$\langle o_3 \rangle \langle o_4 \rangle$	$\langle o_6 \rangle \langle o_4 \rangle$	-	✓
	$\mathbf{S}_{\text{prior}}^{\text{const}}$ (From constant prior knowledge)	$\langle o_1 \rangle \langle o_2 \rangle \langle o_3 \rangle$	$\langle o_1 \rangle \langle o_2 \rangle \langle o_3 \rangle$	$\langle o_1 \rangle \langle o_2 \rangle \langle o_3 \rangle$	-	✓
		$\langle o_4 \rangle \langle o_6 \rangle$	$\langle o_4 \rangle \langle o_6 \rangle$	$\langle o_4 \rangle \langle o_6 \rangle$		

labels are introduced with every task.

Protecting the set of labels is critical in sensitive applications, such as training classification models on medical records from specific hospitals. Exposing labels, e.g. rare diseases, can enable adversaries with prior knowledge to identify individuals in the dataset. For instance, if a rare disease appears in the classifier’s output, it may signal that certain individuals with that disease are included in the dataset. An adversary could then use additional information, such as hospital names and individual addresses, to infer if someone’s data was used in training. Using a public list of general diseases instead mitigates this risk, as it avoids associating labels directly with specific individuals.

In the following, we discuss three possible settings for \mathcal{O}_t as illustrated in Table 1:

\mathbf{S}_{data} : $\mathcal{O}_t := \mathcal{O}_t^{\text{data}}$ or $\mathcal{O}_t := \bigcup_{k=1}^t \mathcal{O}_k^{\text{data}}$, i.e. the true set of labels in task t or the true set of labels from task 1 up to task t . This directly links the classifier output space \mathcal{O}_t with the datasets \mathcal{D}_t .

$\mathbf{S}_{\text{prior}}$: $\mathcal{O}_t := \mathcal{O}_t^{\text{prior}}$, i.e. assumed labels $\mathcal{O}_t^{\text{prior}}$ are provided for each task t . The labels in this case are public, and might or might not match the true set of labels $\mathcal{O}_t^{\text{data}}$. The adversary observes \mathcal{O}_t but not $\mathcal{O}_t^{\text{data}}$.

$\mathbf{S}_{\text{prior}}^{\text{const}}$: $\mathcal{O}_t := \mathcal{O}^{\text{prior}}$, i.e., a constant set which is the set of labels across all tasks that are known publicly before any task. This is a special case of $\mathbf{S}_{\text{prior}}$.

We will next argue that \mathbf{S}_{data} breaks DP (Sec. 4.3), while releasing $\mathbf{S}_{\text{prior}}$ and $\mathbf{S}_{\text{prior}}^{\text{const}}$ do not (Sec. 4.4). Briefly, the reason why \mathbf{S}_{data} is not DP is that the classifier output space is a function of the sensitive dataset, and directly releasing a function of the dataset is not DP. For additional details regarding DP CL mechanisms, see App. F.1.

4.3. Setting \mathbf{S}_{data} Breaks DP

Proposition 4.6. *For any t , the classifier-release mechanism:*

$$\mathcal{M}_t : (\mathcal{D}_t) \mapsto (f_{\theta_t} : \mathcal{X} \rightarrow \mathcal{O}_t) \quad (5)$$

is not (ϵ, δ) -DP for $0 \leq \delta < 1$ if $\mathcal{O}_t = \mathcal{O}_t^{\text{data}}$ or $\mathcal{O}_t = \bigcup_{k=1}^t \mathcal{O}_k^{\text{data}}$, where $\mathcal{O}_t^{\text{data}} = \{y : (\mathbf{x}, y) \in \mathcal{D}_t\}$.

Proof sketch. Consider the counterexample for the mechanism \mathcal{M}_t using two adjacent datasets \mathcal{D}_t and \mathcal{D}'_t , where \mathcal{D}'_t has one more example than \mathcal{D}_t , namely $\{(\mathbf{x}^*, y^*)\}$. It is also assumed that $y^* \in \mathcal{O}'_t$ but $y^* \notin \mathcal{O}_t$. This means that the classifier $\mathcal{M}_t(\mathcal{D}'_t)$ has one more label in its range than $\mathcal{M}_t(\mathcal{D}_t)$. This makes the sets of possible outcomes of $\mathcal{M}_t(\mathcal{D}_t)$ and $\mathcal{M}_t(\mathcal{D}'_t)$ disjoint, which is not DP. The full proof can be found in App. F.2. \square

4.4. Setting $\mathbf{S}_{\text{prior}}$ or $\mathbf{S}_{\text{prior}}^{\text{const}}$ Does Not Break DP

First, we need to re-write Eq. (3) to enable the trusted aggregator to drop the samples that have different labels than $\mathcal{O}_t^{\text{prior}}$ (the set of public labels in task t). We set $\mathcal{O}_t = \mathcal{O}_t^{\text{prior}}$. Let $\mathcal{D}_t^{\text{filtered}}$ denote the set $\{(\mathbf{x}, y) \in \mathcal{D}_t : y \in \mathcal{O}_t\}$, i.e. the set of samples in \mathcal{D}_t that have labels in \mathcal{O}_t . Now, we denote the classifier-release mechanism as:

$$\mathcal{M}_t : (\underbrace{\mathcal{D}_t^{\text{filtered}}}_{\text{private}}, \underbrace{\mathcal{O}_t^{\text{prior}}}_{\text{public}}) \mapsto (f_{\theta_t} : \mathcal{X} \rightarrow \mathcal{O}_t^{\text{prior}}) \quad (6)$$

We show that the mechanism \mathcal{M}_t in Eq. (6) is (ϵ, δ) -DP. The setting $\mathbf{S}_{\text{prior}}^{\text{const}}$ is a special case of this where $\mathcal{O}_t = \mathcal{O}^{\text{prior}}$ for all t .

Proposition 4.7. *For any t , the classifier-release mechanism*

$$\mathcal{M}_t : (\mathcal{D}_t^{\text{filtered}}; \mathcal{O}_t^{\text{prior}}) \mapsto (f_{\theta_t} : \mathcal{X} \rightarrow \mathcal{O}_t^{\text{prior}}) \quad (7)$$

is (ϵ, δ) -DP, if θ_t is obtained by an (ϵ, δ) -DP mechanism from the data $\mathcal{D}_t^{\text{filtered}}$ and labels $\mathcal{O}_t^{\text{prior}}$.

Proof sketch. We show that the mechanism \mathcal{M}_t is (ϵ, δ) -DP by post-processing from the mechanism that provides the DP weights θ_t . We also show that using $\mathcal{D}_t^{\text{filtered}}$ instead of \mathcal{D}_t does not change the privacy guarantees. The full proof can be found in App. F.3. \square

5. DP CL Methods using Pre-Trained Models

We propose two DP methods utilizing pre-trained models.

5.1. Cosine Similarity Classifier

We use the pre-trained model f_{θ}^{pre} as a frozen feature extractor without additional training during CL (Janson et al., 2022) to map images x to feature vectors $v = f_{\theta}^{\text{pre}}(x) \in \mathbb{R}^K$. The basic idea is to accumulate class-specific sums of these vectors under DP, and then classify points according to their cosine similarity with the class sums (see Alg. 1).

At each task $t = 1, \dots, T$, we accumulate a per-class sum of features (normalized to bound the sensitivity of each summand) with the Gaussian mechanism (Balle & Wang, 2018). This will result in a vector $s_{t,o} \in \mathbb{R}^K$ for each of the assumed classes $o \in \mathcal{O}_t$, and writing $s_{0,o} = \mathbf{0}_K$ for any o , we can more generally write:

$$s_{t,o} = \begin{cases} s_{t-1,o} + \left(\sum_{x \in \mathcal{D}_{t,o}} \frac{f_{\theta}^{\text{pre}}(x)}{\|f_{\theta}^{\text{pre}}(x)\|_2} \right) + z_t & \text{if } o \in \mathcal{O}_t \\ s_{t-1,o} & \text{if } o \notin \mathcal{O}_t \end{cases} \quad (8)$$

where $z_t \sim \mathcal{N}(\mathbf{0}, \sigma I)$ is Gaussian noise with scale σ corresponding to the desired (ϵ, δ) -DP privacy budget, $\mathcal{D}_{t,o}$ are all samples from class o at task t , and \mathcal{O}_t is the public set of classes for task t . We compute the sum-of-features rather than the mean-of-features (Janson et al., 2022; Rebuffi et al., 2017) to avoid the need to release the number of examples per class under DP, which would require adding more noise.

To predict the label of a test sample x^* after training up to some time step $t \in \{1, \dots, T\}$, we assign it the class label that maximizes the cosine similarity of v^* with the corresponding per-class feature sum:

$$\hat{y}^* = \arg \max_{o \in \cup_{k=1}^t \mathcal{O}_k} \text{CosineSimilarity}(v^*, s_{t,o}). \quad (9)$$

Note that ℓ_2 -norm and cosine similarity are equivalent when both vectors are normalized to unit norm. Using the ℓ_2 -norm without normalizing is challenging because the magnitude for different sums can vary significantly.

Considering the required amount of memory, we only need to store the per-class sums and the pre-trained model, thus the memory requirements would be $K|\mathcal{O}_t|$ (cumulative sum) + $\dim(\theta)$ (weights pre-trained model). The memory requirements scale as $O(|\cup_{t=1}^T \mathcal{O}_t|)$ growing with the output label space.

5.2. PEFT Ensemble

We construct an ensemble of prediction models by fine-tuning task-specific models f_t on the data set \mathcal{D}_t , $t = 1, \dots, T$ using DP-SGD (see Alg. 2). To avoid having to store T copies of the full model, we can fine-tune either

Algorithm 1 Cosine Classifier

Require: Number of tasks T , per-task DP noise level σ

```

1:  $\mathcal{O}^{\text{seen}} \leftarrow \emptyset$ 
2: for  $t \in [T]$  do
3:   Get task dataset  $\mathcal{D}_t$ 
4:   Get set of labels  $\mathcal{O}_t$  (Assumption  $\mathcal{S}_{\text{prior}}$ )
5:   // Initialize cumulative sums when necessary:
6:   for  $o \in \mathcal{O}_t \setminus \mathcal{O}^{\text{seen}}$  do
7:      $s_o \leftarrow \mathbf{0}$ 
8:   end for
9:    $\mathcal{O}^{\text{seen}} \leftarrow \mathcal{O}^{\text{seen}} \cup \mathcal{O}_t$ 
10:  // Compute DP sum for each  $o \in \mathcal{O}_t$ :
11:  // Add DP sum to cumulative sum:
12:  for  $o \in \mathcal{O}_t$  do
13:     $s_o \leftarrow s_o + \left( \sum_{x \in \mathcal{D}_{t,o}} \frac{f_{\theta}^{\text{pre}}(x)}{\|f_{\theta}^{\text{pre}}(x)\|_2} \right) + \mathcal{N}(0, \sigma I)$ 
14:  end for
15: end for
```

Output: $\{s_1 \dots s_{|\cup_{t=1}^T \mathcal{O}_t|}\}$ (a set of cumulative DP sums)

only the classifier head, or, more generally, use Parameter-Efficient Fine-Tuning (PEFT, Houlsby et al. 2019) with adaptation methods such as LoRA (Hu et al., 2022). In this case, we need to store only the task-specific adapter weights and the final classification layers, as well as a single copy of the pre-trained model. Thus the memory requirements would be $T(|\mathcal{O}_t|K + |\mathcal{O}_t|)$ (last layer) + $T \dim(\theta_{\text{PEFT}})$ (adapter weights) + $\dim(\theta)$ weights pre-trained model. The memory requirements and compute therefore scale as $O((\max_t |\mathcal{O}_t| + \dim(\theta_{\text{PEFT}}))T)$.

The choice of the PEFT fine-tuning method depends on the similarity of pre-training and fine-tuning data. Fine-tuning the last layer only yields a high accuracy when the similarity is high but is computationally more efficient than other PEFT methods (Tobaben et al., 2023). Throughout the paper we employ parameter-efficient FiLM (Perez et al., 2018) adapters, as this approach has been found effective in prior works on transfer learning, including with DP (Shysheya et al., 2023; Tobaben et al., 2023).

Concretely, considering fine-tuning the last layer only, denote the feature vector of the pre-trained model by $v = f_{\theta}^{\text{pre}}(x) \in \mathbb{R}^K$. Then the full task-specific model is $f_t(x) = g_{\phi_t}(v)$, where $g_{\phi_t} : \mathbb{R}^K \rightarrow \mathcal{O}_t$ is the output head with trainable parameters ϕ_t . With FiLM we additionally fine-tune a subset of the backbone normalization layers' parameters of the pre-trained model to shift and scale the activations throughout the backbone. For example, for the model considered in the experiments the FiLM parameters are 0.04% of the total number of pre-trained model parameters.

At test time, say at time $t \in [T]$, we predict the label of a test sample x^* by assigning the class label with the largest

Algorithm 2 PEFT Ensemble

Require: Number of tasks T , DP-SGD parameters ξ

```

1: for  $t \in [T]$  do
2:   Get task dataset  $\mathcal{D}_t$ 
3:   Get set of labels  $\mathcal{O}_t$  (Assumption  $\mathcal{S}_{\text{prior}}$ )
4:   // Initialise model  $f_t$  (predicting label set  $\mathcal{O}_t$ ):
5:    $f_t \leftarrow \text{init}(f_{\theta}^{\text{pre}})$ 
6:   // Train model  $f_t$  with data of the current task  $t$ :
7:    $f_t \leftarrow \text{DP-SGD}(f_t; \mathcal{D}_t, \xi)$ 
8: end for
    
```

Output: $\{f_1 \dots f_T\}$ (a set of T DP models)

logit over all the tasks and all the classes assumed so far¹:

$$\hat{y}^* = \arg \max_{o \in \bigcup_{k=1}^t \mathcal{O}_k, l \in \{1, \dots, t\}} f_l(\mathbf{x}^*, o). \quad (10)$$

In Eq. (10), $f_l(\mathbf{x}^*, o)$ denotes the logit corresponding to label o for the l th model in the ensemble.

6. Experiments

We evaluate how our proposed methods based on pre-trained models (introduced in Sec. 5) perform under varying degrees of domain shift between tasks and pre-training data and between different tasks (Sec. 6.1), with blurry tasks (Sec. 6.2), and given different output label settings ($\mathcal{S}_{\text{prior}}/\mathcal{S}_{\text{prior}}^{\text{const}}$) (Sec. 6.3).

In all experiments, we utilise a ViT-Base-16 (ViT-B) (Dosovitskiy et al., 2021) network pre-trained on the ImageNet-21K (Russakovsky et al., 2015) dataset. We assume that the pre-training data is public and that the task datasets \mathcal{D}_t are sensitive and need to be protected with DP. All experiments are in the class-incremental learning setting where no task labels are available (van de Ven et al., 2022). See App. H for full experimental details.

Datasets We experiment with the following benchmarks for CL: Split-CIFAR-100 which is CIFAR-100 (Krizhevsky, 2009) split into 10 tasks with 10 classes/task. Split-ImageNet-R (Wang et al., 2022a) which is ImageNet-R (Hendrycks et al., 2021) split into 10 tasks with 20 classes/task. 5-Datasets (Ebrahimi et al., 2020) consist of the five data sets, MNIST (LeCun et al., 2010), SVHN (Netzer et al., 2011), notMNIST (Bulatov, 2011), FashionMNIST (Xiao et al., 2017) and CIFAR-10 (Krizhevsky, 2009) where each forms one task.

Metrics We report average accuracies and forgetting metrics from Chaudhry et al. (2018) for evaluation like prior CL work (Mirzadeh et al., 2021; Yoon et al., 2022). The average accuracy measures the test set accuracy across all seen

¹In App. H.2 we consider alternatives to ArgMax including the aggregation rule by Zhao et al. (2024a).

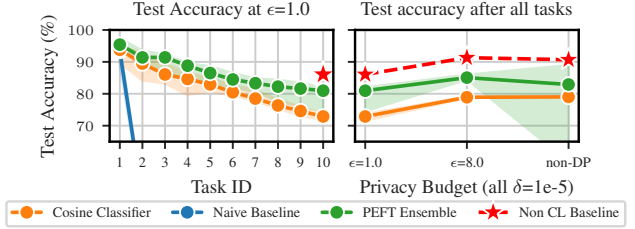


Figure 2. Median test accuracy (error-bars: min/max over 5 seeds) on Split-CIFAR-100. PEFT Ensemble outperforms but Cosine Classifier more stable and viable alternative at given its lower computational requirements.

tasks, while forgetting is given by the difference between the highest accuracy of a task and its accuracy at the current task. See App. H for a formal definition of these metrics.

Baselines We compare against the following baselines:

- **Naive (Lower):** We fine-tune one pre-trained model with DP-SGD over all T tasks sequentially, which is a lower bound as no means to mitigate catastrophic forgetting are in place (See Alg. A2).
- **Non CL Baseline (Upper):** We fine-tune one pre-trained model with DP-SGD with all data $\bigcup_{i=1}^t \mathcal{D}_i$ as an upper bound. This baseline illustrates the cost of DP training without CL (See Alg. A3).

6.1. Varying Degrees of Domain Shift

We experiment with varying degrees of domain shift between tasks and pre-training data and between different tasks. The domain shift between the pre-training data (ImageNet-21k) and Split-CIFAR-100 is smaller than to ImageNet-R or 5-datasets. This influences the difficulty of fine-tuning (Tobaben et al., 2023) (See difference between for last layer and FiLM fine-tuning that is indicative of this shift in Apps. J.1 and J.2). Both Split-CIFAR-100 and ImageNet-R have little domain shift between different tasks as the tasks are only consisting of different classes of the same base dataset whereas the tasks of 5-dataset are consisting of different base datasets. In App. H.2 we compare aggregation rules for the PEFT Ensemble and find that the ArgMax rule outperforms the other aggregation rules.

Split-CIFAR-100 (shift pre-training \rightarrow , shift tasks \rightarrow) Split-CIFAR-100 has small domain shift to the pre-training data and between the tasks. Fig. 2 compares our proposed methods to the baselines with detailed results in App. J.1. The PEFT Ensemble outperforms the Cosine Classifier in all experiments in terms of median accuracy but is more expensive both in storage and compute. Furthermore, the PEFT Ensemble has a larger variability in utility (especially in non-DP due to the overconfidence of models on unseen classes). This makes the Cosine Classifier a viable alternative when storage or compute are limited but the domain shift to the pre-training data is small.

Split-ImageNet-R (shift pre-training ↗, shift tasks →) Split-ImageNet-R has a larger domain shift to the pre-training data than Split-CIFAR-100 but a small shift between tasks. The larger domain shift to the pre-training data further increases the utility gap between the Cosine Classifier and the PEFT Ensemble already observed in the Split-CIFAR-100 experiments as can be seen in Fig. 3. While the classifier performs on-par with prior simple baselines (Jan-son et al., 2022) in the non-DP setting, the PEFT Ensemble achieves 18-20% higher classification accuracy over all privacy budgets. This leads to the $\epsilon = 8$ PEFT Ensemble performing on par with non-DP Cosine Classifier. This suggests that simple baselines that operate in the feature space of the feature extractor are not competitive under DP when the domain shift to the pre-training data is sufficiently large.

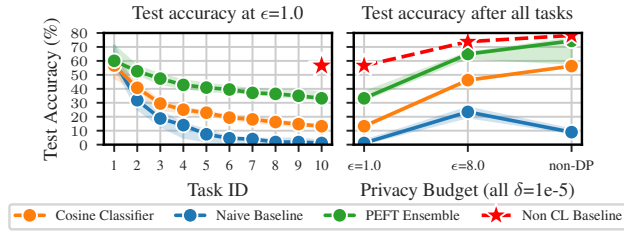


Figure 3. Median test accuracy (error-bars: min/max over 5 seeds) on Split-ImageNet-R. Adaptation of backbone using PEFT Ensemble yields significantly higher test accuracy.

5-Dataset (shift pre-training →, shift tasks ↗) 5-dataset is has the largest shift between the tasks of the three benchmarks. The results for our methods are very similar to the prior observations, we discuss them in App. J.3.

6.2. Blurry Tasks

In Sec. 6.1 each class is only contained in one task but in many real life examples this is not the case. Fig. 4 compares the final test accuracy of our methods in so-called blurry settings of different degree starting not blurry (classes part of one task only), I-Blurry (Koh et al., 2022) (lack of explicit task boundaries for some classes) and SI-Blurry (Moon et al., 2023) (no explicit task boundaries and data imbalance) for Split-CIFAR-100. The Cosine Classifier is unaffected by blurry tasks as it is invariant to the order of feature vectors but the utility of the PEFT Ensemble performs degrades.

6.3. Different Output Label Spaces

Sec. 4.2 introduced different possible settings for determining the output label space of a classifier trained at a particular task t but we used S_{prior}^{const} throughout the prior experiments. Fig. 5 compares the final test accuracy between updating always all labels (S_{prior}^{const}) and an optimal version of S_{prior} that only updates the labels actually being in the data. Under S_{prior} the Cosine Classifier adds a magnitude less noise to the cumulative sum than with S_{prior}^{const} as each class is only

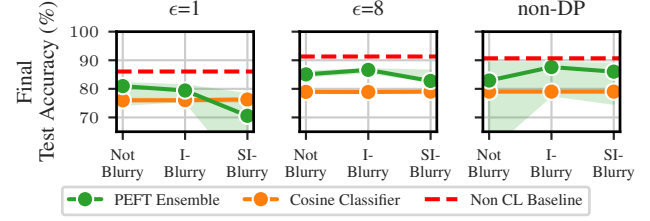


Figure 4. Effect of blurry tasks on our methods for Split-CIFAR-100. Cosine Classifier is unaffected by the task blurriness (constant accuracy) as it is invariant but the PEFT Ensemble is especially effected by the S-I Blurry setting.

part of one of the ten tasks. The utility improves thus in some cases significantly under DP. For the PEFT Ensemble we retrained the individual models with an output layer that is of size 10/20 for S_{prior} in comparison to 100/200 in S_{prior}^{const} but changed nothing else. We only observe a minor effect from this improvement.

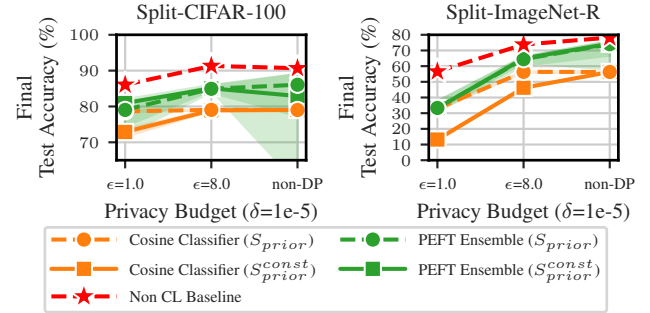


Figure 5. Final test accuracy using S_{prior}^{const} and an optimal version of S_{prior} . S_{prior} mostly results in higher test accuracy for Cosine Classifier due to the decreased amount of DP noise. PEFT Ensemble shows no significant change.

7. Discussion and Conclusion

We formulated the theory for task-wise DP CL and highlighted that the classifiers' output label spaces can lead to catastrophic privacy leakage. Additionally, we developed methods to leverage pre-trained models in DP CL and conducted experiments in the class incremental setting studying the interplay between forgetting, privacy and utility.

Limitations and Future Work We assume that the classes to learn are known at each task which complicates extending DP to online and open-world CL scenarios. Applying DP into methods enabling open-vocabulary classification, e.g., prompt-based methods (Wang et al., 2022b) or vision-language models (Radford et al., 2021), is an interesting direction for tackling this assumption.

The code implementation will be made available on GitHub upon acceptance of the paper.

Acknowledgments

This work was supported by the Research Council of Finland (Flagship programme: Finnish Center for Artificial Intelligence, FCAI, Grant 356499, Grant 359111, and Grant 339730), the Strategic Research Council at the Research Council of Finland (Grant 358247) as well as the European Union (Project 101070617). Views and opinions expressed are however those of the author(s) only and do not necessarily reflect those of the European Union or the European Commission. Neither the European Union nor the granting authority can be held responsible for them. The authors wish to thank the CSC – IT Center for Science, Finland for supporting this project with computational and data storage resources. We thank Rui Li and Aki Rehn for the helpful discussions.

References

- Abadi, M., Chu, A., Goodfellow, I. J., McMahan, H. B., Mironov, I., Talwar, K., and Zhang, L. Deep learning with differential privacy. In *Proceedings of the 2016 ACM SIGSAC Conference on Computer and Communications Security, Vienna, Austria, October 24-28, 2016*, pp. 308–318. ACM, 2016.
- Akiba, T., Sano, S., Yanase, T., Ohta, T., and Koyama, M. Optuna: A next-generation hyperparameter optimization framework. In *Proceedings of the 25th ACM SIGKDD International Conference on Knowledge Discovery & Data Mining, KDD 2019, Anchorage, AK, USA, August 4-8, 2019*, pp. 2623–2631. ACM, 2019.
- Aljundi, R., Lin, M., Goujaud, B., and Bengio, Y. Gradient based sample selection for online continual learning. *Advances in Neural Information Processing Systems*, 32, 2019.
- Balle, B. and Wang, Y. Improving the gaussian mechanism for differential privacy: Analytical calibration and optimal denoising. In *Proceedings of the 35th International Conference on Machine Learning, ICML 2018, Stockholmsmässan, Stockholm, Sweden, July 10-15, 2018*, volume 80 of *Proceedings of Machine Learning Research*, pp. 403–412. PMLR, 2018.
- Balle, B., Cherubin, G., and Hayes, J. Reconstructing training data with informed adversaries. In *43rd IEEE Symposium on Security and Privacy, SP 2022, San Francisco, CA, USA, May 22-26, 2022*, pp. 1138–1156. IEEE, 2022.
- Bulatov, Y. notMNIST dataset, 2011. URL <http://yaroslavvb.blogspot.it/2011/09/notmnist-dataset.html>.
- Cattan, Y., Choquette-Choo, C. A., Papernot, N., and Thakurta, A. Fine-tuning with differential privacy necessitates an additional hyperparameter search. *CoRR*, abs/2210.02156, 2022. doi: 10.48550/arXiv.2210.02156. URL <https://doi.org/10.48550/arXiv.2210.02156>.
- Chaudhry, A., Dokania, P. K., Ajanthan, T., and Torr, P. H. S. Riemannian walk for incremental learning: Understanding forgetting and intransigence. In *Computer Vision - ECCV 2018 - 15th European Conference, Munich, Germany, September 8-14, 2018, Proceedings, Part XI*, volume 11215 of *Lecture Notes in Computer Science*, pp. 556–572. Springer, 2018.
- Chaudhry, A., Rohrbach, M., Elhoseiny, M., Ajanthan, T., Dokania, P. K., Torr, P. H., and Ranzato, M. On tiny episodic memories in continual learning. *arXiv preprint arXiv:1902.10486*, 2019.
- Chen, D., Kerkouche, R., and Fritz, M. Private set generation with discriminative information. In *Advances in Neural Information Processing Systems 35: Annual Conference on Neural Information Processing Systems 2022, NeurIPS 2022, New Orleans, LA, USA, November 28 - December 9, 2022*, 2022.
- Choquette-Choo, C. A., Ganesh, A., Haque, S., Steinke, T., and Thakurta, A. Near Exact Privacy Amplification for Matrix Mechanisms, October 2024. URL <http://arxiv.org/abs/2410.06266>. arXiv:2410.06266 [cs].
- De, S., Berrada, L., Hayes, J., Smith, S. L., and Balle, B. Unlocking high-accuracy differentially private image classification through scale. *ArXiv preprint*, abs/2204.13650, 2022. URL <https://arxiv.org/abs/2204.13650>.
- De Lange, M., Aljundi, R., Masana, M., Parisot, S., Jia, X., Leonardis, A., Slabaugh, G., and Tuytelaars, T. A continual learning survey: Defying forgetting in classification tasks. *IEEE transactions on pattern analysis and machine intelligence*, 44(7):3366–3385, 2021.
- Desai, P., Lai, P., Phan, N., and Thai, M. T. Continual learning with differential privacy. In *Neural Information Processing: 28th International Conference, ICONIP 2021, Sanur, Bali, Indonesia, December 8–12, 2021, Proceedings, Part VI* 28, pp. 334–343. Springer, 2021.
- Dosovitskiy, A., Beyer, L., Kolesnikov, A., Weissenborn, D., Zhai, X., Unterthiner, T., Dehghani, M., Minderer, M., Heigold, G., Gelly, S., Uszkoreit, J., and Houlsby, N. An image is worth 16x16 words: Transformers for image recognition at scale. In *9th International Conference on Learning Representations, ICLR 2021, Virtual Event, Austria, May 3-7, 2021*. OpenReview.net, 2021.

- Douillard, A. and Lesort, T. Continuum: Simple management of complex continual learning scenarios, 2021.
- Dwork, C. and Roth, A. The Algorithmic Foundations of Differential Privacy. *Found. Trends Theor. Comput. Sci.*, 9(3-4):211–407, 2014. ISSN 1551-305X. doi: 10.1561/04000000042. URL <http://dx.doi.org/10.1561/04000000042>.
- Dwork, C., Kenthapadi, K., McSherry, F., Mironov, I., and Naor, M. Our data, ourselves: Privacy via distributed noise generation. In *Advances in Cryptology - EUROCRYPT 2006, 25th Annual International Conference on the Theory and Applications of Cryptographic Techniques, St. Petersburg, Russia, May 28 - June 1, 2006, Proceedings*, volume 4004 of *Lecture Notes in Computer Science*, pp. 486–503. Springer, 2006a.
- Dwork, C., McSherry, F., Nissim, K., and Smith, A. Calibrating noise to sensitivity in private data analysis. In *Theory of Cryptography*, pp. 265–284, Berlin, Heidelberg, 2006b. Springer Berlin Heidelberg.
- Dwork, C., Naor, M., Pitassi, T., Rothblum, G. N., and Yekhanin, S. Pan-Private Streaming Algorithms. In *ics*, pp. 66–80. Tsinghua University Press, 2010a.
- Dwork, C., Rothblum, G. N., and Vadhan, S. P. Boosting and differential privacy. In *51th Annual IEEE Symposium on Foundations of Computer Science, FOCS 2010, October 23-26, 2010, Las Vegas, Nevada, USA*, pp. 51–60. IEEE Computer Society, 2010b.
- Ebrahimi, S., Meier, F., Calandra, R., Darrell, T., and Rohrbach, M. Adversarial continual learning. In *Computer Vision - ECCV 2020 - 16th European Conference, Glasgow, UK, August 23-28, 2020, Proceedings, Part XI*, volume 12356 of *Lecture Notes in Computer Science*, pp. 386–402. Springer, 2020.
- Farquhar, S. and Gal, Y. Differentially private continual learning. *CoRR*, abs/1902.06497, 2019. URL <http://arxiv.org/abs/1902.06497>.
- French, R. M. Catastrophic forgetting in connectionist networks. *Trends in cognitive sciences*, 3(4):128–135, 1999.
- Gao, Q., Zhao, C., Sun, Y., Xi, T., Zhang, G., Ghanem, B., and Zhang, J. A unified continual learning framework with general parameter-efficient tuning. In *IEEE/CVF International Conference on Computer Vision, ICCV 2023, Paris, France, October 1-6, 2023*, pp. 11449–11459. IEEE, 2023.
- Ghalebikesabi, S., Berrada, L., Gawal, S., Ktena, I., Stanforth, R., Hayes, J., De, S., Smith, S. L., Wiles, O., and Balle, B. Differentially private diffusion models generate useful synthetic images. *arXiv preprint arXiv:2302.13861*, 2023.
- Gopi, S., Lee, Y. T., and Wutschitz, L. Numerical composition of differential privacy. In *Advances in Neural Information Processing Systems 34: Annual Conference on Neural Information Processing Systems 2021, NeurIPS 2021, December 6-14, 2021, virtual*, pp. 11631–11642, 2021.
- Granzio, D., Zohren, S., and Roberts, S. Learning rates as a function of batch size: A random matrix theory approach to neural network training. *J. Mach. Learn. Res.*, 23: 173:1–173:65, 2022. URL <https://jmlr.org/papers/v23/20-1258.html>.
- Haim, N., Vardi, G., Yehudai, G., Shamir, O., and Irani, M. Reconstructing training data from trained neural networks. *Advances in Neural Information Processing Systems*, 35: 22911–22924, 2022.
- Hassanpour, A., Moradikia, M., Yang, B., Abdelhadi, A., Busch, C., and Fierrez, J. Differential privacy preservation in robust continual learning. *IEEE Access*, 10: 24273–24287, 2022.
- Hendrycks, D., Basart, S., Mu, N., Kadavath, S., Wang, F., Dorundo, E., Desai, R., Zhu, T., Parajuli, S., Guo, M., et al. The many faces of robustness: A critical analysis of out-of-distribution generalization. In *Proceedings of the IEEE/CVF International Conference on Computer Vision*, pp. 8340–8349, 2021.
- Houlsby, N., Giurigu, A., Jastrzebski, S., Morrone, B., de Laroussilhe, Q., Gesmundo, A., Attariyan, M., and Gelly, S. Parameter-efficient transfer learning for NLP. In *Proceedings of the 36th International Conference on Machine Learning, ICML 2019, 9-15 June 2019, Long Beach, California, USA*, volume 97 of *Proceedings of Machine Learning Research*, pp. 2790–2799. PMLR, 2019.
- Hu, E. J., Shen, Y., Wallis, P., Allen-Zhu, Z., Li, Y., Wang, S., Wang, L., and Chen, W. Lora: Low-rank adaptation of large language models. In *The Tenth International Conference on Learning Representations, ICLR 2022, Virtual Event, April 25-29, 2022*. OpenReview.net, 2022.
- Janson, P., Zhang, W., Aljundi, R., and Elhoseiny, M. A simple baseline that questions the use of pretrained-models in continual learning. *CoRR*, abs/2210.04428, 2022. doi: 10.48550/ARXIV.2210.04428. URL <https://doi.org/10.48550/arXiv.2210.04428>.
- Jung, C., Ligett, K., Neel, S., Roth, A., Sharifi-Malvajerdi, S., and Shenfeld, M. A new analysis of differential privacy’s generalization guarantees (invited paper). In *Proceedings of the 53rd Annual ACM SIGACT Symposium on Theory of Computing, STOC 2021*, pp. 9, New York, NY, USA, 2021. Association for Computing Machinery.

- Koh, H., Kim, D., Ha, J., and Choi, J. Online continual learning on class incremental blurry task configuration with anytime inference. In *The Tenth International Conference on Learning Representations, ICLR 2022, Virtual Event, April 25-29, 2022*. OpenReview.net, 2022.
- Koskela, A. and Kulkarni, T. D. Practical differentially private hyperparameter tuning with subsampling. In *Advances in Neural Information Processing Systems 36: Annual Conference on Neural Information Processing Systems 2023, NeurIPS 2023, New Orleans, LA, USA, December 10 - 16, 2023*, 2023.
- Koskela, A., Jälkö, J., and Honkela, A. Computing tight differential privacy guarantees using FFT. In *The 23rd International Conference on Artificial Intelligence and Statistics, AISTATS 2020, 26-28 August 2020, Online [Palermo, Sicily, Italy]*, volume 108 of *Proceedings of Machine Learning Research*, pp. 2560–2569. PMLR, 2020.
- Koskela, A., Jälkö, J., Prediger, L., and Honkela, A. Tight differential privacy for discrete-valued mechanisms and for the subsampled gaussian mechanism using FFT. In *The 24th International Conference on Artificial Intelligence and Statistics, AISTATS 2021, April 13-15, 2021, Virtual Event*, volume 130 of *Proceedings of Machine Learning Research*, pp. 3358–3366. PMLR, 2021.
- Krizhevsky, A. Learning multiple layers of features from tiny images. Master’s thesis, University of Toronto, 2009.
- Kurakin, A., Chien, S., Song, S., Geambasu, R., Terzis, A., and Thakurta, A. Toward training at imagenet scale with differential privacy. *CoRR*, abs/2201.12328, 2022. URL <https://arxiv.org/abs/2201.12328>.
- Lai, P., Hu, H., Phan, H., Jin, R., Thai, M. T., and Chen, A. M. Lifelong DP: consistently bounded differential privacy in lifelong machine learning. In *Conference on Lifelong Learning Agents, CoLLAs 2022, 22-24 August 2022, McGill University, Montréal, Québec, Canada*, volume 199 of *Proceedings of Machine Learning Research*, pp. 778–797. PMLR, 2022.
- LeCun, Y., Cortes, C., and Burges, C. MNIST handwritten digit database. *ATT Labs [Online]*. Available: <http://yann.lecun.com/exdb/mnist>, 2, 2010.
- Lecuyer, M., Spahn, R., Vodrahalli, K., Geambasu, R., and Hsu, D. Privacy Accounting and Quality Control in the Sage Differentially Private ML Platform, September 2019. URL <http://arxiv.org/abs/1909.01502>. arXiv:1909.01502.
- Li, X., Tramèr, F., Liang, P., and Hashimoto, T. Large language models can be strong differentially private learners. In *The Tenth International Conference on Learning Representations, ICLR 2022, Virtual Event, April 25-29, 2022*. OpenReview.net, 2022.
- Li, Z. and Hoiem, D. Learning without forgetting. *IEEE transactions on pattern analysis and machine intelligence*, 40(12):2935–2947, 2017.
- Lopez-Paz, D. and Ranzato, M. Gradient episodic memory for continual learning. *Advances in Neural Information Processing Systems*, 30, 2017.
- Malladi, S., Lyu, K., Panigrahi, A., and Arora, S. On the sdes and scaling rules for adaptive gradient algorithms. In *Advances in Neural Information Processing Systems 35: Annual Conference on Neural Information Processing Systems 2022, NeurIPS 2022, New Orleans, LA, USA, November 28 - December 9, 2022*, 2022.
- McCloskey, M. and Cohen, N. J. Catastrophic interference in connectionist networks: The sequential learning problem. In *Psychology of learning and motivation*, volume 24, pp. 109–165. Elsevier, 1989.
- McDonnell, M., Gong, D., Parvaneh, A., Abbasnejad, E., and van den Hengel, A. RanPAC: Random projections and pre-trained models for continual learning. In *Thirty-seventh Conference on Neural Information Processing Systems*, 2023.
- McSherry, F. Privacy integrated queries: an extensible platform for privacy-preserving data analysis. *Commun. ACM*, 53(9):89–97, 2010. doi: 10.1145/1810891.1810916. URL <https://doi.org/10.1145/1810891.1810916>.
- Mehta, H., Thakurta, A. G., Kurakin, A., and Cutkosky, A. Towards large scale transfer learning for differentially private image classification. *Trans. Mach. Learn. Res.*, 2023, 2023. URL <https://openreview.net/forum?id=Uu8WwCFpQv>.
- Mirzadeh, S. I., Farajtabar, M., Gorur, D., Pascanu, R., and Ghasemzadeh, H. Linear mode connectivity in multitask and continual learning. In *International Conference on Learning Representations*, 2021.
- Moon, J., Park, K., Kim, J. U., and Park, G. Online class incremental learning on stochastic blurry task boundary via mask and visual prompt tuning. In *IEEE/CVF International Conference on Computer Vision, ICCV 2023, Paris, France, October 1-6, 2023*, pp. 11697–11707. IEEE, 2023.
- Mudrakarta, P. K., Sandler, M., Zhmoginov, A., and Howard, A. G. K for the price of 1: Parameter-efficient multi-task and transfer learning. In *7th International Conference on Learning Representations, ICLR 2019, New Orleans, LA, USA, May 6-9, 2019*. OpenReview.net, 2019.

- Netzer, Y., Wang, T., Coates, A., Bissacco, A., Wu, B., and Ng, A. Y. Reading digits in natural images with unsupervised feature learning. In *NIPS Workshop on Deep Learning and Unsupervised Feature Learning*, 2011.
- Ostapenko, O., Lesort, T., Rodriguez, P., Arefin, M. R., Douillard, A., Rish, I., and Charlin, L. Continual learning with foundation models: An empirical study of latent replay. In *Conference on lifelong learning agents*, pp. 60–91. PMLR, 2022.
- Paszke, A., Gross, S., Massa, F., Lerer, A., Bradbury, J., Chanan, G., Killeen, T., Lin, Z., Gimelshein, N., Antiga, L., Desmaison, A., Köpf, A., Yang, E. Z., DeVito, Z., Raison, M., Tejani, A., Chilamkurthy, S., Steiner, B., Fang, L., Bai, J., and Chintala, S. Pytorch: An imperative style, high-performance deep learning library. In *Advances in Neural Information Processing Systems 32: Annual Conference on Neural Information Processing Systems 2019, NeurIPS 2019, December 8-14, 2019, Vancouver, BC, Canada*, pp. 8024–8035, 2019.
- Patacchiola, M., Bronskill, J., Shysheya, A., Hofmann, K., Nowozin, S., and Turner, R. E. Contextual squeeze-and-excitation for efficient few-shot image classification. In *Advances in Neural Information Processing Systems 35: Annual Conference on Neural Information Processing Systems 2022, NeurIPS 2022, New Orleans, LA, USA, November 28 - December 9, 2022*, 2022.
- Pelikan, M., Azam, S. S., Feldman, V., Silovsky, J. H., Talwar, K., and Likhomanenko, T. Federated learning with differential privacy for end-to-end speech recognition. *CoRR*, abs/2310.00098, 2023. doi: 10.48550/ARXIV.2310.00098. URL <https://doi.org/10.48550/arXiv.2310.00098>.
- Perez, E., Strub, F., de Vries, H., Dumoulin, V., and Courville, A. C. Film: Visual reasoning with a general conditioning layer. In *Proceedings of the Thirty-Second AAAI Conference on Artificial Intelligence, (AAAI-18), the 30th innovative Applications of Artificial Intelligence (IAAI-18), and the 8th AAAI Symposium on Educational Advances in Artificial Intelligence (EAAI-18), New Orleans, Louisiana, USA, February 2-7, 2018*, pp. 3942–3951. AAAI Press, 2018.
- Ponomareva, N., Hazimeh, H., Kurakin, A., Xu, Z., Denison, C., McMahan, H. B., Vassilvitskii, S., Chien, S., and Thakurta, A. G. How to dp-fy ML: A practical guide to machine learning with differential privacy. *J. Artif. Intell. Res.*, 77:1113–1201, 2023. doi: 10.1613/JAIR.1.14649. URL <https://doi.org/10.1613/jair.1.14649>.
- Radford, A., Kim, J. W., Hallacy, C., Ramesh, A., Goh, G., Agarwal, S., Sastry, G., Askell, A., Mishkin, P., Clark, J., et al. Learning transferable visual models from natural language supervision. In *International Conference on Machine Learning*, pp. 8748–8763, 2021.
- Rajkumar, A. and Agarwal, S. A differentially private stochastic gradient descent algorithm for multiparty classification. In *Proceedings of the Fifteenth International Conference on Artificial Intelligence and Statistics, AISTATS 2012, La Palma, Canary Islands, Spain, April 21-23, 2012*, volume 22 of *JMLR Proceedings*, pp. 933–941. JMLR.org, 2012.
- Rasmussen, C. E. and Williams, C. K. I. *Gaussian processes for machine learning*. Adaptive computation and machine learning. MIT Press, 2006. ISBN 026218253X. URL <https://www.worldcat.org/oclc/61285753>.
- Rebuffi, S.-A., Kolesnikov, A., Sperl, G., and Lampert, C. H. icarl: Incremental classifier and representation learning. In *Proceedings of the IEEE Conference on Computer Vision and Pattern Recognition*, pp. 2001–2010, 2017.
- Russakovsky, O., Deng, J., Su, H., Krause, J., Satheesh, S., Ma, S., Huang, Z., Karpathy, A., Khosla, A., Bernstein, M., Berg, A. C., and Fei-Fei, L. ImageNet Large Scale Visual Recognition Challenge. *International Journal of Computer Vision (IJCV)*, 115(3):211–252, 2015. doi: 10.1007/s11263-015-0816-y.
- Shokri, R., Stronati, M., Song, C., and Shmatikov, V. Membership inference attacks against machine learning models. In *2017 IEEE Symposium on Security and Privacy, SP 2017, San Jose, CA, USA, May 22-26, 2017*, pp. 3–18. IEEE Computer Society, 2017.
- Shysheya, A., Bronskill, J., Patacchiola, M., Nowozin, S., and Turner, R. E. FiT: parameter efficient few-shot transfer learning for personalized and federated image classification. In *The Eleventh International Conference on Learning Representations, ICLR 2023, Kigali, Rwanda, May 1-5, 2023*. OpenReview.net, 2023.
- Song, S., Chaudhuri, K., and Sarwate, A. D. Stochastic gradient descent with differentially private updates. In *IEEE Global Conference on Signal and Information Processing, GlobalSIP 2013, Austin, TX, USA, December 3-5, 2013*, pp. 245–248. IEEE, 2013.
- Thiel, D. Identifying and eliminating csam in generative ml training data and models. Technical report, Technical Report. Stanford University, Palo Alto, CA., 2023. URL <https://purl.stanford.edu/kh752sm9123>.
- Tito, R., Nguyen, K., Tobaben, M., Kerkouche, R., Souibgui, M. A., Jung, K., Kang, L., Valveny, E., Honkela, A., Fritz, M., and Karatzas, D. Privacy-aware document visual question answering. *CoRR*, abs/2312.10108, 2023.

- doi: 10.48550/ARXIV.2312.10108. URL <https://doi.org/10.48550/arXiv.2312.10108>.
- Tobaben, M., Shysheya, A., Bronskill, J., Pavard, A., Tople, S., Béguelin, S. Z., Turner, R. E., and Honkela, A. On the efficacy of differentially private few-shot image classification. *Transactions on Machine Learning Research*, 2023. ISSN 2835-8856. URL <https://openreview.net/forum?id=hFsr59Imzm>.
- Tramèr, F., Kamath, G., and Carlini, N. Position: Considerations for differentially private learning with large-scale public pretraining. In *Forty-first International Conference on Machine Learning, ICML 2024, Vienna, Austria, July 21-27, 2024*. OpenReview.net, 2024.
- van de Ven, G. M., Tuytelaars, T., and Tolias, A. S. Three types of incremental learning. *Nat. Mac. Intell.*, 4(12): 1185–1197, 2022. doi: 10.1038/S42256-022-00568-3. URL <https://doi.org/10.1038/s42256-022-00568-3>.
- Wahdany, D., Jagielski, M., Dziedzic, A., and Boenisch, F. Beyond the mean: Differentially private prototypes for private transfer learning. *arXiv preprint arXiv:2406.08039*, 2024.
- Wang, L., Zhang, X., Su, H., and Zhu, J. A comprehensive survey of continual learning: theory, method and application. *IEEE Transactions on Pattern Analysis and Machine Intelligence*, 2024.
- Wang, Z., Zhang, Z., Ebrahimi, S., Sun, R., Zhang, H., Lee, C.-Y., Ren, X., Su, G., Perot, V., Dy, J., et al. Dualprompt: Complementary prompting for rehearsal-free continual learning. In *European Conference on Computer Vision*, pp. 631–648. Springer, 2022a.
- Wang, Z., Zhang, Z., Lee, C., Zhang, H., Sun, R., Ren, X., Su, G., Perot, V., Dy, J. G., and Pfister, T. Learning to prompt for continual learning. In *IEEE/CVF Conference on Computer Vision and Pattern Recognition, CVPR 2022, New Orleans, LA, USA, June 18-24, 2022*, pp. 139–149. IEEE, 2022b.
- Whitehouse, J., Ramdas, A., Rogers, R., and Wu, S. Fully-adaptive composition in differential privacy. In *International Conference on Machine Learning, ICML 2023, 23-29 July 2023, Honolulu, Hawaii, USA*, volume 202 of *Proceedings of Machine Learning Research*, pp. 36990–37007. PMLR, 2023.
- Xiao, H., Rasul, K., and Vollgraf, R. Fashion-MNIST: a novel image dataset for benchmarking machine learning algorithms. *CoRR*, abs/1708.07747, 2017. URL <http://arxiv.org/abs/1708.07747>.
- Xu, Z., Zhang, Y., Andrew, G., Choquette-Choo, C. A., Kairouz, P., McMahan, H. B., Rosenstock, J., and Zhang, Y. Federated learning of gboard language models with differential privacy. In *Proceedings of the The 61st Annual Meeting of the Association for Computational Linguistics: Industry Track, ACL 2023, Toronto, Canada, July 9-14, 2023*, pp. 629–639. Association for Computational Linguistics, 2023.
- Yoon, J., Yang, E., Lee, J., and Hwang, S. J. Lifelong learning with dynamically expandable networks. In *International Conference on Learning Representations*, 2018.
- Yoon, J., Madaan, D., Yang, E., and Hwang, S. J. Online coreset selection for rehearsal-based continual learning. In *International Conference on Learning Representations*, 2022.
- Yousefpour, A., Shilov, I., Sablayrolles, A., Testuggine, D., Prasad, K., Malek, M., Nguyen, J., Gosh, S., Bharadwaj, A., Zhao, J., Cormode, G., and Mironov, I. Opacus: User-friendly differential privacy library in pytorch. *ArXiv preprint*, abs/2109.12298, 2021. URL <https://arxiv.org/abs/2109.12298>.
- Yu, D., Naik, S., Backurs, A., Gopi, S., Inan, H. A., Kamath, G., Kulkarni, J., Lee, Y. T., Manoel, A., Wutschitz, L., Yekhanin, S., and Zhang, H. Differentially private fine-tuning of language models. In *The Tenth International Conference on Learning Representations, ICLR 2022, Virtual Event, April 25-29, 2022*. OpenReview.net, 2022.
- Zhang, J., Zhang, Z., Xiao, X., Yang, Y., and Winslett, M. Functional mechanism: Regression analysis under differential privacy. *CoRR*, abs/1208.0219, 2012. URL <http://arxiv.org/abs/1208.0219>.
- Zhao, L., Zhang, X., Yan, K., Ding, S., and Huang, W. SAFE: slow and fast parameter-efficient tuning for continual learning with pre-trained models. *CoRR*, abs/2411.02175, 2024a. doi: 10.48550/ARXIV.2411.02175. URL <https://doi.org/10.48550/arXiv.2411.02175>.
- Zhao, L., Zhang, X., Yan, K., Ding, S., and Huang, W. Safe: Slow and fast parameter-efficient tuning for continual learning with pre-trained models. In *The Thirty-eighth Annual Conference on Neural Information Processing Systems*, 2024b.
- Zhou, D.-W., Cai, Z.-W., Ye, H.-J., Zhan, D.-C., and Liu, Z. Revisiting class-incremental learning with pre-trained models: Generalizability and adaptivity are all you need. *International Journal of Computer Vision*, pp. 1–21, 08 2024a. doi: 10.1007/s11263-024-02218-0.

Zhou, D.-W., Sun, H.-L., Ye, H.-J., and Zhan, D.-C.
Expandable subspace ensemble for pre-trained model-
based class-incremental learning. In *Proceedings of the
IEEE/CVF Conference on Computer Vision and Pattern
Recognition*, pp. 23554–23564, 2024b.

Appendices

A. Notation

Table A1. Notations

t	task index
T	total number of tasks
I	set of task indices
$\text{units}(\mathcal{D}_t)$	a mapping that provides the privacy unit of a dataset
$\mathbf{x}_t^{(i)}$	i th sample features in task t
$y_t^{(i)}$	i th sample label in task t
N_t	total number of samples in task t
m	input data dimensionality
$\mathcal{X}, (\mathcal{X}_t)$	(task-specific) feature space
$\mathcal{O}, (\mathcal{O}_t)$	(task-specific) general output space
$\mathcal{O}^{\text{data}}, (\mathcal{O}_t^{\text{data}})$	true (task-specific) label space
$\mathcal{O}^{\text{prior}}, (\mathcal{O}_t^{\text{prior}})$	publicly known (task-specific) label set
$\mathcal{D}, (\mathcal{D}_t)$	(task-specific) data set (features and labels)
ε, δ	DP privacy parameters
$\mathcal{D} \simeq \mathcal{D}'$	DP neighboring datasets
\mathcal{A}	randomized algorithm
$\text{Range}(\mathcal{A})$	set of all possible outcomes for \mathcal{A}
S	outcome event for a randomized algorithm
\mathcal{M}_t	DP algorithm for releasing the classifier in task t
\mathcal{M}	DP algorithm for composing the classifiers for tasks $1 \dots T$
θ	model parameters
f_{θ}^{pre}	pre-trained model parameterized by θ
f_{θ}	classifier parameterized by θ
\mathbf{S}_{data}	setting where the dataset labels are directly released
$\mathbf{S}_{\text{prior}}$	setting where public labels are used for each task
$\mathbf{S}_{\text{prior}}^{\text{const}}$	setting where all the labels are known prior to any task
$s_{t,o}$	noisy feature sum for task t , class o
K	feature extractor dimensionality (omitting classifier layer)
$\mathbf{v} = f_{\theta}^{\text{pre}}(\mathbf{x}) \in \mathbb{R}^K$	feature vector from pre-trained model
$\mathcal{D}_{t,o}$	samples with class o in task t
ξ	General DP-SGD parameters
$g_{\phi_t} : \mathbb{R}^K \rightarrow \mathcal{O}_t$	task-specific head parameterized by ϕ_t
$\mathbf{z}_t \sim \mathcal{N}(\mathbf{0}, \sigma I)$	Gaussian noise with scale σ

B. Detailed Discussion on Existing DP CL Definitions

In this section we discuss in more detail how our formal definition of task-wise DP connects to the existing work, and how considering this definition of DP CL clarifies and fills up the gaps in the existing DP CL theory. As a reminder, task-wise DP requires each \mathcal{M}_t to be (ϵ, δ) -DP separately and the neighborhood relation is given by $\mathcal{D}_t \simeq \mathcal{D}'_t$.

Unlike the earlier work, [Desai et al. \(2021\)](#) define DP specifically for CL. However, as we argue in the following, their stated definitions leave important gaps in the theory and lead to some avoidable complications. In short, the main issue with their formal approach is the following adjacency relation for DP CL (written here using notation compatible with this work):

Definition B.1 (Definition 2 in [Desai et al. 2021](#)). Two databases $D = (\mathcal{D}, M)$ and $D' = (\mathcal{D}', M')$, where $\mathcal{D} = \cup_{i=1}^N \mathcal{D}_i$, $\mathcal{D}' = \cup_{i=1}^N \mathcal{D}'_i$ are data sets, $M = \cup_{i=1}^N M_i$, $M' = \cup_{i=1}^N M'_i$ are memory buffers, are called continual adjacent, if $\|\mathcal{D} - \mathcal{D}'\|_1 \leq 1$ and $\|M - M'\|_1 \leq 1$.

In the following, we exclude M from the database definition, as we do not allow any examples to be stored (no memory

buffer).² The database adjacency then boils down to the adjacency of \mathcal{D} and \mathcal{D}' only. Despite the fact that Definition B.1 only considers the union over all tasks, Desai et al. (2021) actually do privacy accounting for each task separately, and then calculate the total privacy over all tasks through basic sequential composition: $\varepsilon = \sum_{t=1}^T \varepsilon_t$ (Desai et al., 2021, Lemmas 1 & 2). The problem is that assuming $\|\mathcal{D} - \mathcal{D}'\|_1 \leq 1$ as in Definition B.1 is not equivalent to $\|\mathcal{D}_t - \mathcal{D}'_t\|_1 \leq 1$ for all $t = 1, \dots, T$, which is necessary for the task-level privacy accounting used by Desai et al. (2021): with $T > 1$ we can obviously choose $\mathcal{D}_t, \mathcal{D}'_t$, e.g., s.t. $\mathcal{D}_t \cap \mathcal{D}'_t = \emptyset, t = 1, \dots, T$, while still satisfying $\|\cup_t \mathcal{D}_t - \cup_t \mathcal{D}'_t\|_1 \leq 1$.³ As a result, such DP bounds can be invalid as the true privacy loss can be considerably larger than stated, depending on the actual task-level datasets. Instead, starting from the task-level adjacencies $\mathcal{D}_t \simeq \mathcal{D}'_t, t = 1, \dots, T$ as we propose, we can account for valid DP bounds for each task-specific mechanism \mathcal{M}_t , as well as for $(\mathcal{M}_1, \dots, \mathcal{M}_T)$, where the resulting bounds depend on the type of composition we assume over the tasks (see App. C for details).

Instead of defining DP specifically for CL, Hassanpour et al. (2022) use a DP definition for data streams (the rough idea is that neighboring streams of data differ by a single element, see Dwork et al. 2010a; Lecuyer et al. 2019). While this definition can provide meaningful DP guarantees in the CL setting we consider (these guarantees, however, are different and weaker from the guarantees under our proposed task-wise DP), it also presents problems which Hassanpour et al. (2022) do not consider: the main issue in this case is privacy accounting when using DP-SGD on a task level while the adjacency is defined on the level of data streams. This causes issues with sub-sampling amplification, which typically assumes that each minibatch of data is sampled iid from a larger dataset (see, e.g., the discussion on amplification with streaming adjacency by Choquette-Choo et al. 2024). For this reason, the streaming adjacency is not well-suited for our proposed approaches.

For Lifelong learning with DP (Lifelong DP), Lai et al. (2022) propose a model that combines an auto-encoder with a multi-layer neural network classifier. This provides better re-usability, as the auto-encoder can be re-used for different predictive models. The DP mechanism they propose is based on the Functional Mechanism (Zhang et al., 2012) which perturbs the Taylor approximations of the reconstruction function and classification loss function. In particular, they apply the Laplace Mechanism to perturb the coefficients of the Taylor approximations of these functions. Any post-processing applied afterwards to any of these function such as computing gradients is, thus, private. Applying gradient updates to the model parameters is also a post-processing step, which makes the composition of these updates parallel. This also permits the release of intermediate model parameters, i.e. for each task separately. Although, they propose a task level adjacency relation for the ϵ -Lifelong learning it is only limited to parallel composition as the privacy budget can not increase according to Definition B.2. On the other hand, task-wise DP allows potentially any composition method.

Definition B.2 (Definition 3 in Lai et al. 2022). ϵ -Lifelong DP. Given a lifelong database data_m , a randomized algorithm A achieves ϵ -Lifelong DP, if for any of two lifelong neighboring databases $(\text{data}_m, \text{data}'_m)$, for all possible outputs $\{\theta^i\}_{i \in [1, m]} \in \text{Range}(A), \forall m \in [1, \infty)$ we have that

$$P[A(\text{data}_m) = \{\theta^i\}_{i \in [1, m]}] \leq e^\epsilon P[A(\text{data}'_m)_{i \in [1, m]} = \{\theta^i\}_{i \in [1, m]}] \quad (\text{A1})$$

$$\nexists (\epsilon' < \epsilon, i \leq m) : P[A(\text{data}_i) = \{\theta^i\}_{j \in [1, i]}] \leq e^{\epsilon'} P[A(\text{data}'_i) = \{\theta^j\}_{j \in [1, i]}] \quad (\text{A2})$$

where $\text{Range}(A)$ denotes every possible output of A .

B.1. Task-Wise DP Adjacency Relation

For this discussion, denote $|I|$ as T . In task-wise DP (Definition 4.1), we introduced the adjacency relation on the task-level, such that for all $t \in I, \|\mathcal{D}_t - \mathcal{D}'_t\|_1 \leq 1$. This adjacency relation, however, is not equivalent to the adjacency relation that is typically introduced in the streaming setting where $\mathcal{D} = \bigcup_{t \in I} \mathcal{D}_t$ and $\mathcal{D}' = \bigcup_{t \in I} \mathcal{D}'_t$ for two reasons:

1. For task-wise DP, under the streaming setting, it holds that $\|\mathcal{D} - \mathcal{D}'\|_1 \leq T$ and not $\|\mathcal{D} - \mathcal{D}'\|_1 \leq 1$.
2. Although $\|\mathcal{D} - \mathcal{D}'\|_1 \leq T$ for task-wise DP under the streaming setting, the task-level adjacency introduces additional structure such that in each task t , \mathcal{D}_t can only differ from its neighboring dataset \mathcal{D}'_t in at most one sample. While in other streaming-based adjacency relations, such as in Desai et al. (2021) and Hassanpour et al. (2022), it is not clear how the adjacency relation in the data streams $\mathcal{D} \simeq \mathcal{D}'$ translate to the task level and is usually left ambiguous.

To impose the additional structure from task-wise DP in the streaming setting, the adjacency relation $\|\mathcal{D} - \mathcal{D}'\|_1 \leq T$ is not sufficient to capture this subtlety, since additional information is required to derive each \mathcal{D}'_t from \mathcal{D}' . Instead, given any

²We note that including M as in Definition B.1 would not fix the issues discussed in this section.

³For a concrete example with add/remove adjacency, let $\mathcal{D}_t = \{x_{t,1}, \dots, x_{t,N_t}\}, t = 1, \dots, T$ with some samples $x_{i,t}$ that are unique over all tasks, $\mathcal{D}'_t = \mathcal{D}_{t+1}, t = 1, \dots, T-1$ and $\mathcal{D}'_T = \mathcal{D}_1 \cup \{x^*\}$ with x^* again unique.

datasets $(\mathcal{D}_t)_{t \in I}$, we define a new dataset \mathbb{D} such that:

$$\mathbb{D} = \prod_{t \in I} \mathcal{D}_t,$$

i.e., \mathbb{D} is the Cartesian product of the task datasets \mathcal{D}_t . Define the projection function $\pi_t : \mathbb{D} \rightarrow \mathcal{D}_t$ as

$$\pi_t(\mathbf{d}) = \pi_t((d_i)_{i \in I}) = d_t, \quad (\text{A3})$$

where $\mathbf{d} = (d_i)_{i \in I} \in \mathbb{D}$ and $d_t \in \mathcal{D}_t$. Note that $\pi_t(\mathbb{D}) = \mathcal{D}_t$. If we assume that

$$\mathbb{D}' = \mathbb{D} \cup \{(d_i^*)_{i \in I}\}, \quad (\text{A4})$$

then \mathbb{D} differs from \mathbb{D}' by one element, which is the tuple $\mathbf{d}^* = (d_i^*)_{i \in I}$. If we define $\mathcal{D}'_t = \pi_t(\mathbb{D}')$, and the neighborhood relation on \mathbb{D} is then the typical neighborhood relation in DP, which implies the following:

$$\|\mathbb{D} - \mathbb{D}'\|_1 \leq 1 \implies \|\pi_t(\mathbb{D}) - \pi_t(\mathbb{D}')\|_1 = \|\mathcal{D}_t - \mathcal{D}'_t\|_1 \leq 1 \quad (\text{A5})$$

If \mathcal{M}_t is (ϵ, δ) -DP for all t , define $\mathbb{M}_t = \mathcal{M}_t \circ \pi_t$ (the composition of \mathcal{M}_t and π_t), so $\mathbb{M}_t(\mathbb{D}) = \mathcal{M}_t(\pi_t(\mathbb{D})) = \mathcal{M}_t(\mathcal{D}_t)$. Furthermore, defining the composition of the mechanisms $(\mathbb{M}_i)_{i \in I}$ as

$$\mathbb{M} : (\mathbb{D}) \mapsto (\mathbb{M}_i(\mathbb{D}))_{i \in I}, \quad (\text{A6})$$

shows that it is possible to write down the composition of the mechanisms \mathcal{M}_t using \mathbb{D} .

C. Composition under Task-Wise DP

If the list of mechanisms $(\mathcal{M}_t)_{t=1}^T$ is task-wise (ϵ, δ) -DP, we want to compute the (ϵ, δ) -DP privacy guarantees for:

$$\mathcal{M} : (\mathcal{D}_t)_{t \in I} \mapsto (\mathcal{M}_t(\mathcal{D}_t))_{t \in I}. \quad (\text{A7})$$

If $\text{units}(\mathcal{D}_i) \cap \text{units}(\mathcal{D}_j) = \emptyset$ for all $i \neq j$, then according to [Theorem 4.4](#), \mathcal{M} is (ϵ, δ) -DP where $T = |I|$. The worst-case privacy guarantee for \mathcal{M} is $(T\epsilon, T\delta)$ -DP. To see this, consider [Theorem 4.5](#) and Theorem 3.16 of [\(Dwork & Roth, 2014\)](#). Both adaptive and fully adaptive composition can be applied to the result in [Theorem 4.5](#) to obtain better privacy guarantees for \mathcal{M} .

C.1. Proof of Lemma 4.3

Proof. Let $\mathcal{D} \simeq \mathcal{D}'$ be any adjacent datasets, then for any t , setting $\mathcal{D}_t = \mathcal{D}$ and $\mathcal{D}'_t = \mathcal{D}'$, and applying the statement of [Definition 4.1](#), we obtain that for any $S \subseteq \text{Range}(\mathcal{M}_t)$:

$$\Pr[\mathcal{M}_t(\mathcal{D}) \in S] \leq \exp(\epsilon) \times \Pr[\mathcal{M}_t(\mathcal{D}') \in S] + \delta. \quad (\text{A8})$$

Hence, \mathcal{M}_t is (ϵ, δ) -DP according to [Definition 3.1](#). \square

C.2. Proof of Theorem 4.4

Proof. First, [Lemma 4.3](#) implies that \mathcal{M}_t is (ϵ, δ) -DP for all t . Let $\mathcal{D} = \bigcup_{t \in I} \mathcal{D}_t$ for any sets $(\mathcal{D}_t)_{t \in I}$, and let $\mathcal{D}' \simeq \mathcal{D}$ be a neighboring dataset. Assume without loss of generality, that \mathcal{D}' has one more sample than \mathcal{D} such that $\mathcal{D}' = \mathcal{D} \cup \{(\mathbf{x}^*, y^*)\}$ and $\text{units}(\{(\mathbf{x}^*, y^*)\}) \cap \mathcal{D} = \emptyset$, then $(\mathbf{x}^*, y^*) \notin \mathcal{D}$ (by contraposition). We can write \mathcal{D}' as

$$\mathcal{D}' = \bigcup_{t \in I \setminus \{t^*\}} \mathcal{D}_t \cup (\mathcal{D}_{t^*} \cup \{(\mathbf{x}^*, y^*)\}) \quad (\text{A9})$$

for any $t^* \in I$. Define $\mathcal{D}'_t = \mathcal{D}_t$ for all $t \neq t^*$ and $\mathcal{D}'_{t^*} = \mathcal{D}_{t^*} \cup \{(\mathbf{x}^*, y^*)\}$. Thus, $\mathcal{D}' = \bigcup_{t \in I} \mathcal{D}'_t$.

To satisfy the condition of the theorem, assume that $\text{units}(\mathcal{D}_i) \cap \text{units}(\mathcal{D}_j) = \emptyset$ for all $i \neq j$. This implies that $\mathcal{D}_i \cap \mathcal{D}_j = \emptyset$ and $\mathcal{D}'_i \cap \mathcal{D}'_j = \emptyset$ for all $i \neq j$ (by contraposition).

From the fact that $\mathcal{D}_t = \mathcal{D} \cap \mathcal{D}_t = \mathcal{D} \cap \mathcal{D}'_t$ for all t , then it also holds that:

$$\mathcal{M}_t(\mathcal{D}_t) = \mathcal{M}_t(\mathcal{D} \cap \mathcal{D}_t) = \mathcal{M}_t(\mathcal{D} \cap \mathcal{D}'_t). \quad (\text{A10})$$

Moreover,

$$\mathcal{M}_t(\mathcal{D}'_t) = \mathcal{M}_t(\mathcal{D}' \cap \mathcal{D}'_t). \quad (\text{A11})$$

Define the mechanisms $\mathcal{A}_t(\cdot) = \mathcal{M}_t(\cdot \cap \mathcal{D}'_t)$ for all t . Thus,

$$\mathcal{A}_t(\mathcal{D}) = \mathcal{M}_t(\mathcal{D}_t), \quad (\text{A12})$$

and

$$\mathcal{A}_t(\mathcal{D}') = \mathcal{M}_t(\mathcal{D}'_t), \quad (\text{A13})$$

for all t . In particular, for $t \neq t^*$, $\mathcal{D}'_t = \mathcal{D}_t$, and thus $\mathcal{A}_t(\mathcal{D}'_t) = \mathcal{A}_t(\mathcal{D}_t)$ for $t \neq t^*$. Since, for all t , \mathcal{M}_t is (ϵ, δ) -DP, then \mathcal{A}_t is (ϵ, δ) -DP for all t . Hence, for $t = t^*$ and for all $S_{t^*} \subseteq \text{Range}(\mathcal{A}_{t^*})$,

$$\Pr[\mathcal{A}_{t^*}(\mathcal{D}) \in S_{t^*}] \leq \exp(\epsilon) \times \Pr[\mathcal{A}_{t^*}(\mathcal{D}') \in S_{t^*}] + \delta \quad (\text{A14})$$

Define \mathcal{A} as the composition:

$$\mathcal{A}(\cdot) = (\mathcal{A}_t(\cdot))_{t \in I}. \quad (\text{A15})$$

Let $S \subseteq \text{Range}(\mathcal{M})$, where \mathcal{M} is the composition defined in Eq. (4). Denote $S_t = \pi_t(S)$, where

$$\pi_t : \prod_{k \in I} \text{Range}(\mathcal{M}_k) \rightarrow \text{Range}(\mathcal{M}_t) \quad (\text{A16})$$

is the composition projection function, such that $\pi_t((f_k)_{k \in I}) = f_t$. Therefore,

$$\begin{aligned} \Pr[\mathcal{M}((\mathcal{D}_t)_{t \in I}) \in S] &= \Pr[\mathcal{A}(\mathcal{D}) \in S] \\ &= \prod_{t \in I} \Pr[\mathcal{A}_t(\mathcal{D}) \in S_t] \\ &= \prod_{t \in I \setminus \{t^*\}} \Pr[\mathcal{A}_t(\mathcal{D}') \in S_t] \times \Pr[\mathcal{A}_{t^*}(\mathcal{D}) \in S_{t^*}] \\ &\leq \prod_{t \in I \setminus \{t^*\}} \Pr[\mathcal{A}_t(\mathcal{D}') \in S_t] \times (\exp(\epsilon) \times \Pr[\mathcal{A}_{t^*}(\mathcal{D}') \in S_{t^*}] + \delta) \\ &= \exp(\epsilon) \times \prod_{t \in I} \Pr[\mathcal{A}_t(\mathcal{D}') \in S_t] + \delta \times \prod_{t \in I \setminus \{t^*\}} \Pr[\mathcal{A}_t(\mathcal{D}') \in S_t] \\ &= \exp(\epsilon) \times \Pr[\mathcal{A}(\mathcal{D}') \in S] + \delta \times \prod_{t \in I \setminus \{t^*\}} \Pr[\mathcal{A}_t(\mathcal{D}') \in S_t] \\ &\leq \exp(\epsilon) \times \Pr[\mathcal{A}(\mathcal{D}') \in S] + \delta \\ &= \exp(\epsilon) \times \Pr[\mathcal{M}((\mathcal{D}'_t)_{t \in I}) \in S] + \delta, \end{aligned} \quad (\text{A17})$$

because the product of probabilities is less than 1. Since \mathcal{A} is then (ϵ, δ) -DP, then also \mathcal{M} is (ϵ, δ) -DP which ends the proof. \square

C.3. Proof of Theorem 4.5

Proof. First, Lemma 4.3 implies that \mathcal{M}_t is (ϵ, δ) -DP for all t . Let $\mathcal{D} = \bigcup_{t \in I} \mathcal{D}_t$ for any sets $(\mathcal{D}_t)_{t \in I}$, and let $\mathcal{D}' \simeq \mathcal{D}$ be a neighboring dataset. Assume without loss of generality, that \mathcal{D}' has one more sample than \mathcal{D} such that $\mathcal{D}' = \mathcal{D} \cup \{(\mathbf{x}^*, y^*)\}$. We can write \mathcal{D}' as

$$\mathcal{D}' = \bigcup_{t \in I \setminus \{t^*\}} \mathcal{D}_t \cup (\mathcal{D}_{t^*} \cup \{(\mathbf{x}^*, y^*)\}) \quad (\text{A18})$$

for any $t^* \in I$. Define $\mathcal{D}'_t = \mathcal{D}_t$ for all $t \neq t^*$ and $\mathcal{D}'_{t^*} = \mathcal{D}_{t^*} \cup \{(\mathbf{x}^*, y^*)\}$. Thus, $\mathcal{D}' = \bigcup_{t \in I} \mathcal{D}'_t$.

From the fact that $\mathcal{D}_t = \mathcal{D} \cap \mathcal{D}_t = \mathcal{D} \cap \mathcal{D}'_t$ for all t , then it also holds that:

$$\mathcal{M}_t(\mathcal{D}_t) = \mathcal{M}_t(\mathcal{D} \cap \mathcal{D}_t) = \mathcal{M}_t(\mathcal{D} \cap \mathcal{D}'_t). \quad (\text{A19})$$

Moreover,

$$\mathcal{M}_t(\mathcal{D}'_t) = \mathcal{M}_t(\mathcal{D}' \cap \mathcal{D}'_t). \quad (\text{A20})$$

Define the mechanisms $\mathcal{A}_t(\cdot) = \mathcal{M}_t(\cdot \cap \mathcal{D}'_t)$ for all t . Thus,

$$\mathcal{A}_t(\mathcal{D}) = \mathcal{M}_t(\mathcal{D}_t), \quad (\text{A21})$$

and

$$\mathcal{A}_t(\mathcal{D}') = \mathcal{M}_t(\mathcal{D}'_t), \quad (\text{A22})$$

for all t . In particular, for $t \neq t^*$, $\mathcal{D}'_t = \mathcal{D}_t$, and thus $\mathcal{A}_t(\mathcal{D}'_t) = \mathcal{A}_t(\mathcal{D}_t)$ for $t \neq t^*$. Since, for all t , \mathcal{M}_t is (ϵ, δ) -DP, then \mathcal{A}_t is (ϵ, δ) -DP for all t . Additionally, define \mathcal{A} as the composition:

$$\mathcal{A}(\cdot) = (\mathcal{A}_t(\cdot))_{t \in I}. \quad (\text{A23})$$

Hence, $\mathcal{M}((\mathcal{D}_t)_{t \in I}) = \mathcal{A}(\mathcal{D}) = (\mathcal{A}_t(\mathcal{D}))_{t \in I}$, and $\mathcal{M}((\mathcal{D}'_t)_{t \in I}) = \mathcal{A}(\mathcal{D}') = (\mathcal{A}_t(\mathcal{D}'))_{t \in I}$.

Therefore, \mathcal{M} is the sequential composition of $T = |I|$ (ϵ, δ) -DP mechanisms, which are $(\mathcal{A}_t)_{t \in I}$. Non-adaptive or adaptive sequential composition results from [Dwork & Roth \(2014\)](#); [Dwork et al. \(2010b\)](#); [Whitehouse et al. \(2023\)](#) can be applied on \mathcal{A} with the neighbors $\mathcal{D} \simeq \mathcal{D}'$ to obtain the final privacy guarantees. \square

D. Background on Differentially Private Deep Learning

D.1. Differentially private stochastic gradient descent (DP-SGD)

The most straightforward way of training deep learning models under DP is using DP-SGD which clips per-example gradients and adds noise to the aggregate. [Alg. A1](#) displays DP-SGD. There are many implementations of DP-SGD but we use the established implementation in the PyTorch ([Paszke et al., 2019](#)) compatible library opacus ([Yousefpour et al., 2021](#)).

Algorithm A1 Differentially private stochastic gradient descent (DP-SGD)([Rajkumar & Agarwal, 2012](#); [Song et al., 2013](#); [Abadi et al., 2016](#))

Hyper-parameters: learning rate η_t , noise multiplier σ^2 , lot size L , clipping bound C , number of steps T

```

1: for  $t \in [T]$  do
2:   Take a random sample  $L_t$  with sampling probability  $L/N$ 
3:   Compute (per example) gradients
4:   For each  $i \in L_t$  compute  $g_t(x_i) \leftarrow \nabla_{\theta_t} \mathcal{L}(\theta_t, x_i)$ 
5:   Clip gradients
6:    $\tilde{g}_t(x_i) \leftarrow g_t(x_i) / \max(1, \frac{\|g_t(x_i)\|_2}{C})$ 
7:   Add noise
8:    $\tilde{g}_t \leftarrow \frac{1}{|L_t|} (\sum_i \tilde{g}_t(x_i) + \mathcal{N}(0, \sigma^2 C^2 I))$ 
9:   Descent
10:   $\theta_{t+1} = \theta_t - \eta_t \tilde{g}_t$ 
11: end for
```

Output: θ_T and overall privacy cost (ϵ, δ) computed using a privacy accountant.

D.1.1. PRIVACY ACCOUNTING

DP-SGD introduces a trade-off between privacy and utility. Stronger privacy guarantees require introducing more noise, which proportionately degrades model accuracy. (ϵ, δ) -DP ([Dwork et al., 2006a](#)) has a privacy budget consisting of $\epsilon \geq 0$ and $\delta \in [0, 1]$, where smaller values of each correspond to a stronger privacy guarantee.

The privacy guarantee of a DP-SGD run is based on the hyper-parameters used for running DP-SGD and can be quantified using privacy accountants ([Koskela et al., 2020; 2021; Gopi et al., 2021](#)). The following hyper-parameters have an influence on the privacy guarantee of DP-SGD:

- **Number of steps T :** Training for more iterations results in a lower privacy guarantee.
- **Sampling probability L/N :** A higher sampling probability increases the probability that a sample will be used for computing gradients at an iteration t and thus results in a lower privacy guarantee.
- **Noise multiplier σ^2 :** A higher noise multiplier σ^2 results in a higher privacy guarantee.

The learning rate η does not influence the privacy guarantee as it only scales the final update that is already DP. The clipping bound C is an important hyperparameter in DP-SGD but it is not influencing the privacy guarantee as a higher clipping bound C will also lead to more noise being added to the aggregation the gradient as can be seen in line 8 of Alg. A1. One needs to adjust the clipping bound C in a way that not too much information is lost due to the clipping of gradients but at the same time not too much noise is added to aggregate.

E. Appendix: DP CL Theory main text original version

F. DP + CL for Classification Theory Details

F.1. Other Details Related to DP CL Mechanisms

A necessary condition for \mathcal{M} in Eq. (4) to be DP is that it should not leak that any of the task datasets is empty, *i.e.* that $\mathcal{D}_t = \emptyset$ (almost surely) for some t . Let \perp mean that the aggregator did not provide a classifier. We also say that \perp is not a “proper” classifier. If $\mathcal{M}_t(\mathcal{D}_t) = \perp$ (almost surely) when $\mathcal{D}_t = \emptyset$ and $\mathcal{M}_t(\mathcal{D}_t) \neq \perp$ (almost surely) when $\mathcal{D}_t \neq \emptyset$, then \mathcal{M} is not DP according to Proposition F.1. The reason is that this can potentially leak whether the classifier was trained including or excluding a certain sample. Therefore, we will assume that the classifier release mechanism always outputs a proper classifier $\mathcal{M}_t(\mathcal{D}_t) \neq \perp$ (almost surely) for any t . In practice, for the case of using pretrained models, when $\mathcal{D}_t = \emptyset$, we can initialize both the fine-tuning weights and the classifier’s weights randomly before releasing the classifier.

Proposition F.1. *The mechanism \mathcal{M}_t is not (ϵ, δ) -DP for $0 \leq \delta < 1$ when $\mathcal{M}_t(\mathcal{D}_t) = \perp$ (almost surely) if and only if $\mathcal{D}_t = \emptyset$.*

Denote the range of \mathcal{M}_t as $\mathcal{H}_t \cup \{\perp\}$, *i.e.* the union of the hypothesis space \mathcal{H}_t (proper-classifiers) and $\{\perp\}$ (non-proper classifier). For the following proof, note that $\perp \notin \mathcal{H}_t$ for any t .

Proof. We argue by constructing a counterexample. Assume that \mathcal{M}_t is (ϵ, δ) -DP for $0 \leq \delta < 1$ and that $\mathcal{M}_t(\mathcal{D}_t) = \perp$ (almost surely) iff $\mathcal{D}_t = \emptyset$. Let $\mathcal{D}_t = \emptyset$ and $\mathcal{D}'_t = \{(\mathbf{x}^*, y^*)\}$ where $(\mathbf{x}^*, y^*) \in \mathcal{X} \times \mathcal{O}_t$ is arbitrary. Since \mathcal{M}_t is (ϵ, δ) -DP, then for all $S \subseteq \mathcal{H}_t$,

$$\Pr[\mathcal{M}(\mathcal{D}'_t) \in S] \leq e^\epsilon \Pr[\mathcal{M}(\mathcal{D}_t) \in S] + \delta. \quad (\text{A24})$$

Let $S = \mathcal{H}_t$, then

$$\Pr[\mathcal{M}(\mathcal{D}'_t) \in S] = 1. \quad (\text{A25})$$

However, since $\mathcal{D}_t = \emptyset$, then $\mathcal{M}_t(\mathcal{D}_t) = \perp \notin \mathcal{H}_t$. Thus,

$$\Pr[\mathcal{M}(\mathcal{D}_t) \in S] = 0. \quad (\text{A26})$$

Therefore, Eq. (A24) implies that

$$1 \leq e^\epsilon \times 0 + \delta \implies 1 \leq \delta, \quad (\text{A27})$$

but we assumed that $0 < \delta < 1$, a contradiction. \square

F.2. Proof of Proposition 4.6

For the following proof, let $\pi_{\mathcal{Y}} : \mathcal{X} \times \mathcal{Y} \rightarrow \mathcal{Y}$ be the label projection function where \mathcal{Y} is the space of all possible labels, *i.e.* $\pi_{\mathcal{Y}}(\mathbf{x}, y) = y$ for any $(\mathbf{x}, y) \in \mathcal{D}_t$.

Proof. We argue by constructing a counterexample. Assume that \mathcal{M}_t is (ϵ, δ) -DP for $0 \leq \delta < 1$. Let \mathcal{D}_t and \mathcal{D}'_t be any two datasets that differ in only one example such that $\mathcal{D}'_t = \mathcal{D}_t \cup \{(\mathbf{x}^*, y^*)\}$. If either $\mathcal{O}_t = \mathcal{O}_t^{\text{data}}$ or $\mathcal{O}_t = \bigcup_{k=1}^t \mathcal{O}_k^{\text{data}}$, then

$$\pi_{\mathcal{Y}}(\mathcal{D}_t) \subseteq \mathcal{O}_t. \quad (\text{A28})$$

Let $\text{Range}(\cdot)$ be the mapping that takes a function as an input and outputs its range, *i.e.* $\text{Range}(f : A \rightarrow B) = B$. Denote $\mathcal{O}'_t = \text{Range}(\mathcal{M}_t(\mathcal{D}'_t))$. For the counter example, since \mathcal{O}'_t also contains $\pi_{\mathcal{Y}}(\mathcal{D}'_t)$, then assume that $y^* \in \mathcal{O}'_t$, and assume that $y^* \notin \mathcal{O}_t$. Note that $\text{Range}(\mathcal{M}_t(\mathcal{D}_t))$ is a post-processing from $\mathcal{M}_t(\mathcal{D}_t)$, and thus it is also (ϵ, δ) -DP. Hence, for any $S \subseteq \mathcal{O}_t^{\text{data}}$,

$$\Pr[\text{Range}(\mathcal{M}_t(\mathcal{D}'_t)) \in S] \leq e^\epsilon \Pr[\text{Range}(\mathcal{M}_t(\mathcal{D}_t)) \in S] + \delta. \quad (\text{A29})$$

Equivalently,

$$\Pr[\mathcal{O}'_t \in S] \leq e^\epsilon \Pr[\mathcal{O}_t \in S] + \delta. \quad (\text{A30})$$

Let $S = \{\mathcal{O}'_t\}$. Since $y^* \notin \mathcal{O}_t$, then $\mathcal{O}'_t \neq \mathcal{O}_t$. This implies that,

$$\Pr[\mathcal{O}'_t \in S] = 1, \quad (\text{A31})$$

and that

$$\Pr[\mathcal{O}_t \in S] = 0. \quad (\text{A32})$$

From Eqs. (A30) to (A32), we obtain

$$1 \leq e^\epsilon \times 0 + \delta \implies 1 \leq \delta, \quad (\text{A33})$$

but we assumed that $0 < \delta < 1$, a contradiction. \square

Proposition 4.6 can be generalized to any function

$$\mathcal{U} : \mathcal{X} \times \mathcal{Y} \rightarrow \mathcal{Y},$$

such that there exists two neighboring datasets \mathcal{D}_t and \mathcal{D}'_t that differ in only one example and $\mathcal{U}(\mathcal{D}_t) \neq \mathcal{U}(\mathcal{D}'_t)$. Thus, setting $\mathcal{O}_t = \mathcal{U}(\bigcup_{k=1}^t \mathcal{D}_k)$ or $\mathcal{O}_t = \mathcal{U}(\mathcal{D}_t)$, a counterexample can be constructed as in the proof of Proposition 4.6.

F.3. Proof of Proposition 4.7

Proof. Define \mathcal{W} to be (ϵ, δ) -DP mechanism that provides the weights θ_t . In other words,

$$\theta_t = \mathcal{W}(\mathcal{D}_t^{\text{filtered}}; \mathcal{O}_t^{\text{prior}}). \quad (\text{A34})$$

To show that using $\mathcal{D}_t^{\text{filtered}}$ instead of \mathcal{D}_t does not change the privacy guarantees for \mathcal{W} , let \mathcal{D}_t be any set and $\mathcal{D}'_t \simeq \mathcal{D}_t$. Assume without the loss of generality that $\mathcal{D}'_t = \mathcal{D}_t \cup \{(\mathbf{x}^*, y^*)\}$, *i.e.* that \mathcal{D}'_t has an additional point. There are two possibilities for $(\mathcal{D}'_t)^{\text{filtered}}$:

1. $(\mathcal{D}'_t)^{\text{filtered}} = \mathcal{D}_t^{\text{filtered}}$, that is when $y \notin \mathcal{O}_t^{\text{prior}}$
2. $(\mathcal{D}'_t)^{\text{filtered}} = \mathcal{D}_t^{\text{filtered}} \cup \{(\mathbf{x}, y)\}$, that is when $y \in \mathcal{O}_t^{\text{prior}}$

First, if $(\mathcal{D}'_t)^{\text{filtered}} = \mathcal{D}_t^{\text{filtered}}$, then it is trivial that for all $S \subseteq \text{Range}(\mathcal{W})$:

$$\Pr[\mathcal{W}(\mathcal{D}_t^{\text{filtered}}; \mathcal{O}_t^{\text{prior}}) \in S] \leq \exp(\epsilon) \times \Pr[\mathcal{W}((\mathcal{D}'_t)^{\text{filtered}}; \mathcal{O}_t^{\text{prior}}) \in S] + \delta. \quad (\text{A35})$$

Second, if $(\mathcal{D}'_t)^{\text{filtered}} = \mathcal{D}_t^{\text{filtered}} \cup \{(\mathbf{x}, y)\}$, then since \mathcal{W} is an (ϵ, δ) -DP mechanism, setting $\mathcal{D} = \mathcal{D}_t^{\text{filtered}}$ and $\mathcal{D}' = (\mathcal{D}'_t)^{\text{filtered}}$ in Definition 3.1, we obtain

$$\Pr[\mathcal{W}(\mathcal{D}_t^{\text{filtered}}; \mathcal{O}_t^{\text{prior}}) \in S] \leq \exp(\epsilon) \times \Pr[\mathcal{W}((\mathcal{D}'_t)^{\text{filtered}}; \mathcal{O}_t^{\text{prior}}) \in S] + \delta. \quad (\text{A36})$$

Therefore, in both cases, using $\mathcal{D}_t^{\text{filtered}}$ does not change the privacy guarantees of \mathcal{W} . Finally, since \mathcal{W} is (ϵ, δ) -DP, then the mechanism

$$\mathcal{M}_t(\mathcal{D}_t^{\text{filtered}}; \mathcal{O}_t^{\text{prior}}) := f_{\mathcal{W}(\mathcal{D}_t^{\text{filtered}}; \mathcal{O}_t^{\text{prior}})} : \mathcal{X} \rightarrow \mathcal{O}_t^{\text{prior}} \quad (\text{A37})$$

is a post-processing from \mathcal{W} , and thus is also (ϵ, δ) -DP. \square

G. Baseline Details

Below, we provide pseudo-codes for the baselines introduced in Sec. 6.

G.1. Naive Baseline

We start training a model f at task $t = 1$ under DP and continue further training it for all tasks T using DP-SGD. This is a lower bound as no measures are in place to mitigate catastrophic forgetting.

Algorithm A2 Naive Baseline

```

1: Initialise model  $f$ 
2:  $f \leftarrow \text{init}()$ 
3: for  $t \in [T]$  do
4:   Continue to train the model with the data of the current task  $t$ 
5:    $f \leftarrow \text{DP-SGD}(f; D_t)$ 
6: end for
Output: a set of  $T$  model checkpoints  $\{f_1 \dots f_T\}$  (note that this is for evaluating)

```

Test of the models

```

1: for  $t \in [T]$  do
2:   Predict test data of all tasks seen so far
3:   for  $x_i^* \in \cup_i^t \mathcal{D}_i^{\text{test}}$  do
4:      $\hat{y}_i^* \leftarrow \arg \max_k f_t(x_i^*)$ 
5:   end for
6:   Evaluate average accuracy and forgetting
7:   average accuracy $_t$ , forgetting $_t \leftarrow \text{eval}(\{y_i \dots\}, \{y_i^* \dots\}, \text{per-task accuracy history})$ 
8: end for

```

Output: average accuracy for all tasks T $\{\text{average accuracy}_1 \dots \text{average accuracy}_T\}$, average forgetting for all tasks T $\{\text{forgetting}_1 \dots \text{forgetting}_T\}$

G.2. Full Data Baseline

We assume the availability $\cup_i^t \mathcal{D}_i$ and train a model with DP-SGD (Abadi et al., 2016). While this is DP it is not CL.

Algorithm A3 Full Data Baseline

Training of the model

```

1: Initialise model  $f$ 
2:  $f \leftarrow \text{init}()$ 
3: Train a model with all the data
4:  $f \leftarrow \text{DP-SGD}(f; \cup_i^T D_i)$ 

```

Output: a model f

Test of the models

```

1: Predict test data
2: for  $x_i^* \in \cup_i^T \mathcal{D}_i^{\text{test}}$  do
3:    $\hat{y}_i^* \leftarrow \arg \max_k f(x_i^*)$ 
4: end for
5: Evaluate average accuracy
6: average accuracy  $\leftarrow \text{eval}(\{y_i \dots\}, \{y_i^* \dots\})$ 

```

Output: average accuracy

H. Experimental Details

Pre-trained Model Throughout all experiments, we utilise a Vision Transformer ViT-Base-16 (ViT-B) (Dosovitskiy et al., 2021) with 85.8M parameters, pretrained on the ImageNet-21K (Russakovsky et al., 2015) dataset. We assume that the pre-training data (ImageNet-21K) is public, and the downstream data \mathcal{D} is private and needs to be protected with DP.

For all methods but the Cosine Classifier we fine-tune the pre-trained model. We set the weights of the last linear layer of the ViT-B to zero and always learn them when fine-tuning on \mathcal{D} . Additionally, we employ Parameter-Efficient Fine-Tuning in some experiments by learning FiLM (Perez et al., 2018) layers. Although there are many other such adapters such as Model Patch (Mudrakarta et al., 2019), LoRA (Hu et al., 2022), CaSE (Patacchiola et al., 2022) *etc.*, we chose FiLM as it has proven to be highly effective in prior works on (DP) parameter-efficient few-shot transfer learning (Shysheya et al., 2023; Tobaben et al., 2023). The number of FiLM parameters for the ViT-B are 38400 as we implement it by freezing all weights but the layer norm scale and bias weights. The the number of the last layer in comparison are $768C + C$ weights, so for example for Split-CIFAR-100 we fine-tune $38400 + 76900 = 115300$ parameters in the $\mathbf{S}_{\text{prior}}^{\text{const}}$ setting.

We implement our methods using PyTorch (Paszke et al., 2019), continuum (Douillard & Lesort, 2021), and opacus (Yousefpour et al., 2021) with the PRV accounting (Gopi et al., 2021).

Metrics We report the average accuracy and the average forgetting as (Chaudhry et al., 2018; Mirzadeh et al., 2021; Yoon et al., 2022):

- **Accuracy:** The average accuracy at task t is defined as

$$\text{average accuracy}_t = \frac{1}{t} \sum_{i=1}^t \text{test set accuracy}_{t,i} \in [0, 1], \quad (\text{A38})$$

where test set accuracy $_{t,i} \in [0, 1]$ is the test set accuracy for task i after learning task t . Note that average accuracy $_T$ is the average accuracy across all tasks after the final task T has been learned.

- **Forgetting:** The forgetting of task i is defined as the difference between its highest accuracy and its accuracy at the current task t as

$$\text{forgetting}_{t,i} = \max_{k \in \{1, \dots, t-1\}} (\text{test set accuracy}_{k,i} - \text{test set accuracy}_{t,i}) \in [-1, 1], \quad (\text{A39})$$

such that the average forgetting at task t is then given by

$$\text{average forgetting}_t = \frac{1}{t-1} \sum_{i=1}^{t-1} \text{forgetting}_{t,i} \in [-1, 1]. \quad (\text{A40})$$

Note that average forgetting $_T$ is the average forgetting across the first $T - 1$ tasks as there is no forgetting of the final learned task T .

Data sets We experiment with the following data sets:

- **Split CIFAR-100:** Split CIFAR-100 which is CIFAR-100 (Krizhevsky, 2009) split into 10 tasks with 10 classes/task. We randomly permute the class order for each seed we run.
- **5-Datasets:** This data set concatenates the five 10-class data sets, MNIST (LeCun et al., 2010), SVHN (Netzer et al., 2011), notMNIST (Bulatov, 2011), FashionMNIST (Xiao et al., 2017) and CIFAR-10 (Krizhevsky, 2009). Each data set is considered a task, such that there are 5 tasks with 10 classes/task. We run experiments with all permutations of the tasks.
- **Split ImageNet-R:** This data set consists 30,000 images of renditions (art, cartoons, etc.) of 200 ImageNet classes (Hendrycks et al., 2021) and was introduced by Wang et al. (2022a) as a benchmark for CL with pre-trained models. As in (Janson et al., 2022; Wang et al., 2022a), we split the classes into 10 tasks with 20 classes/task. We make a random 80/20% train/test split across the whole dataset. The samples per class are imbalanced in the original data set, and we obtain a 41-334 samples/class in our training sets with our split.

H.1. Hyperparameters

We tune the hyperparameters for the DP-SGD methods for each combination of privacy budget (ϵ, δ) and seed once using the hyperparameter tuning library Optuna (Akiba et al., 2019) with the Gaussian process (Rasmussen & Williams, 2006) sampler for 20 iterations. The ranges for the hyperparameters can be found in Table A2.

Table A2. Hyperparameter ranges used for the tuning.

	LOWER BOUND	UPPER BOUND
EPOCHS		40
LEARNING RATE	1E-7	1E-2
BATCH SIZE	10	TUNING DATASET SIZE
CLIPPING NORM	0.2	10
NOISE MULTIPLIER	BASED ON TARGET ϵ	

The tuning is done using a smaller subset than the final training dataset to reduce the required compute budget. For the 5-dataset datasets (CIFAR-10, FashionMNIST, MNIST, notMNIST and SVHN) we tune using a subset of CIFAR-10 that is 10% the size of the final training dataset and select the hyperparameters that yield the best validation accuracy on a validation dataset of size 4.28% of the final training dataset. For Split-CIFAR-100 and ImageNet-R we tune using a dataset that is representative of one task (10/20 classes) by splitting the representative dataset 70:30 into tuning and validation dataset. For all datasets, we linearly scale the (expected) batch size to keep the subsampling ratio constant for the new training dataset size (Koskela & Kulkarni, 2023) and scale the learning rate of Adam by $\sqrt{\text{scaling_factor}}$ as suggested by prior work (Granziol et al., 2022; Malladi et al., 2022). We do not scale the clipping bound and keep the number of epochs constant at 40.

Similarly to prior work (De et al., 2022; Mehta et al., 2023; Tobaben et al., 2023) we do not account for additional privacy budget spending during the tuning of the hyperparameters.

H.2. PEFT Ensemble Aggregation Rules

We also compared two other aggregation rules in Fig. A.1 to the aggregation rule introduced in Eq. (10), which we refer to as ArgMax. The Median aggregation rule is obtained by subtracting the median of the logits for each model separately, given by the following equation:

$$\hat{y}^* = \arg \max_{o \in \bigcup_{k=1}^t \mathcal{O}_k, l \in \{1, \dots, t\}} \left(f_l(\mathbf{x}^*, o) - \text{median}_{o' \in \bigcup_{k=1}^t \mathcal{O}_k} f_l(\mathbf{x}^*, o') \right). \quad (\text{A41})$$

We additionally implement the entropy-based aggregation rule proposed by (Zhao et al., 2024a) in Equation (11), using the recommended parameter value $\gamma = 1$ from Section 4.1, which is further supported by the ablation study in Appendix D. We refer to this aggregation rule as Entropy.

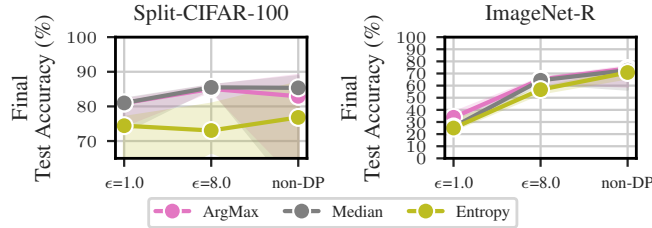


Figure A.1. Median accuracy comparison between ArgMax (Eq. (10)), Median (Eq. (A41)), and Entropy (Equation (11) of Zhao et al. (2024a)) aggregation rules for the PEFT model Ensemble. The error bars are the min/max accuracies obtained over five repeats with different class ordering, hyperparameter tuning runs and DP noise.

I. Licenses and Access

The Vision Transformer ViT-Base-16 (ViT-B) (Dosovitskiy et al., 2021) is licensed with the Apache-2.0 license and can be obtained through the instructions on https://github.com/google-research/vision_transformer.

The licenses and means to access the data sets can be found below. We downloaded all data sets but notMNIST and ImageNet-R from torchvision (version 0.18.1).

- CIFAR10 (Krizhevsky, 2009) is licensed with an unknown license and the data set as specified on <https://pytorch.org/vision/main/generated/torchvision.datasets.CIFAR10.html#torchvision.datasets.CIFAR10>.
- CIFAR100 (Krizhevsky, 2009) is licensed with an unknown license and we the data set as specified on <https://pytorch.org/vision/stable/generated/torchvision.datasets.CIFAR100.html#torchvision.datasets.CIFAR100>.
- FashionMNIST (Xiao et al., 2017) is licensed under MIT and we use the data set as specified on <https://pytorch.org/vision/stable/generated/torchvision.datasets.FashionMNIST.html#torchvision.datasets.FashionMNIST>.
- ImageNet-R (Hendrycks et al., 2021) is licensed with an unknown license and we use the version from <https://people.eecs.berkeley.edu/~hendrycks/imagenet-r.tar>.
- MNIST (LeCun et al., 2010) is licensed with an unknown license and we the data set as specified on <https://pytorch.org/vision/stable/generated/torchvision.datasets.MNIST.html#torchvision.datasets.MNIST>.
- notMNIST (Bulatov, 2011) is licensed under an unknown license and we use the version at git hash 339df59 found at <https://github.com/facebookresearch/Adversarial-Continual-Learning/blob/main/data/notMNIST.zip>
- SVHN (Netzer et al., 2011) is licensed under CC and the data set as specified on <https://pytorch.org/vision/stable/generated/torchvision.datasets.SVHN.html#torchvision.datasets.SVHN>.

J. Detailed Results

In this section we provide detailed tabular results and additional figures for the experiments in Sec. 6.

J.1. Split-CIFAR-100

This subsection complements the results of Fig. 2.

Table A3. Average accuracy (AA) and average forgetting (AF) (scaled by 100) after learning the final task in % on 10-task Split-CIFAR-100. We report the mean and std of the metrics averaged over 5 seeds. We did not compute the AF numbers of the naive baseline at other privacy levels than $\epsilon = 1$ as the performance is expected to be bad.

Method	$\epsilon = 1, \delta = 1e-5$		$\epsilon = 8, \delta = 1e-5$		non-DP	
	AA (\uparrow)	AF (\downarrow)	AA (\uparrow)	AF (\downarrow)	AA (\uparrow)	AF (\downarrow)
Naive	9.35 \pm 0.14	94.10 \pm 0.00	9.55 \pm 0.23	-	9.63 \pm 0.05	-
Cosine classifier	72.78 \pm 0.51	9.92 \pm 0.51	78.93 \pm 0.10	6.15 \pm 0.24	79.02 \pm 0.00	6.02 \pm 0.56
PEFT Ensemble (FiLM)	79.79 \pm 3.02	7.17 \pm 2.56	85.26 \pm 0.633	6.07 \pm 0.59	79.39 \pm 12.20	10.43 \pm 9.28
Non CL Baseline (FiLM)	86.06	-	91.31	-	90.68	-
PEFT Ensemble (last layer)	78.81 \pm 0.48	0.06 \pm 0.00	82.48 \pm 0.31	-	82.60 \pm 0.38	-
Non CL Baseline (last layer)	85.1	-	88.5	-	88.4	-

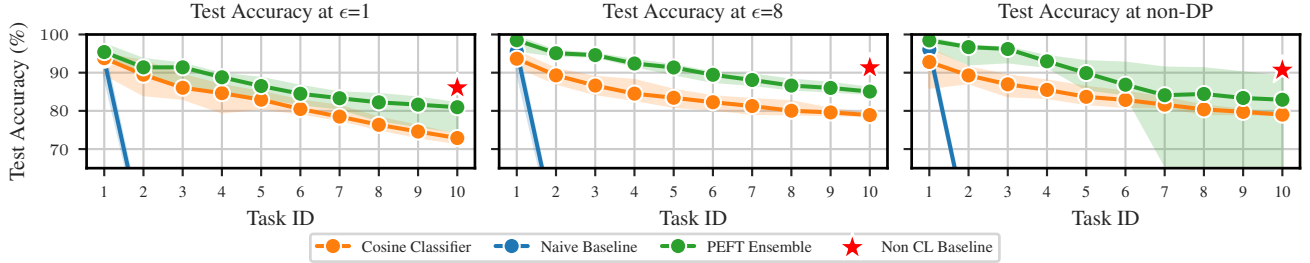


Figure A.2. Median test accuracy per task on Split-CIFAR-100 (ViT-B pre-trained on ImageNet-21k). The error bars are the min/max accuracies obtained over five repeats with different class ordering, hyperparameter tuning runs and DP noise.

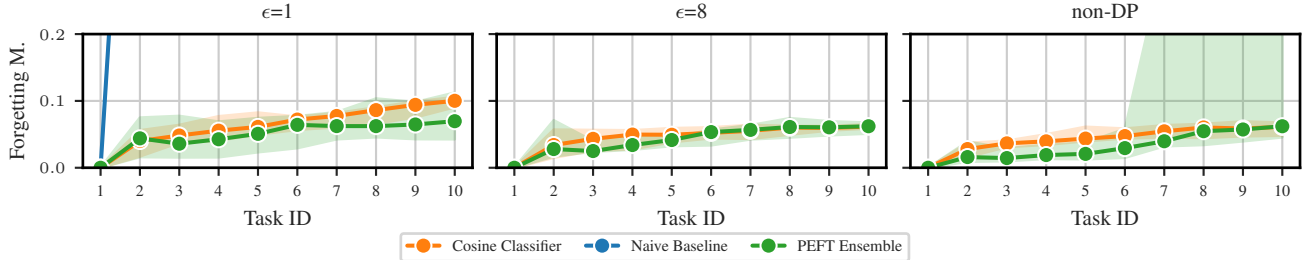


Figure A.3. Median forgetting measure per task on Split-CIFAR-100 (ViT-B pre-trained on ImageNet-21k). The error bars are the min/max forgetting measure obtained over five repeats with different class ordering, hyperparameter tuning runs and DP noise.

J.2. ImageNet-R

This subsection complements the results of Fig. 3.

Table A4. Average accuracy (AA) and average forgetting (AF) (scaled by 100) after learning the final task in % on 10-task Split ImageNet-R. We report the mean and std of the metrics averaged over three seeds.

Method	$\epsilon = 1, \delta = 1e-5$		$\epsilon = 8, \delta = 1e-5$		non-DP	
	AA (\uparrow)	AF (\downarrow)	AA (\uparrow)	AF (\downarrow)	AA (\uparrow)	AF (\downarrow)
Naive	1.52 ± 0.79	37.90 ± 8.05	23.49 ± 2.50	66.92 ± 1.94	9.12 ± 0.99	87.51 ± 1.59
Cosine classifier	13.04 ± 1.23	13.89 ± 2.97	46.17 ± 0.21	12.21 ± 2.15	56.30 ± 0.00	7.51 ± 1.49
PEFT Ensemble (FiLM)	33.19 ± 2.37	12.22 ± 2.30	64.91 ± 1.75	8.87 ± 0.93	74.32 ± 7.63	6.07 ± 1.11
Non CL Baseline (FiLM)	56.62	-	73.77	-	78.24	-
PEFT Ensemble (last layer)	7.29 ± 2.82	3.54 ± 0.62	47.97 ± 2.22	6.33 ± 0.72	48.16 ± 12.80	6.54 ± 4.19
Non CL Baseline (last layer)	16.57 ± 2.86	-	52.16 ± 4.35	-	62.17 ± 2.03	-

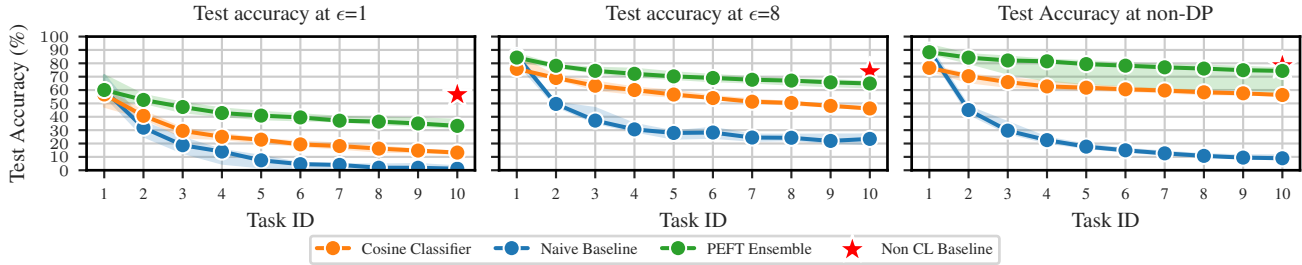


Figure A.4. Median test accuracy per task on ImageNet-R (ViT-B pre-trained on ImageNet-21k). The error bars are the min/max accuracies obtained over five repeats with different class ordering, hyperparameter tuning runs and DP noise.

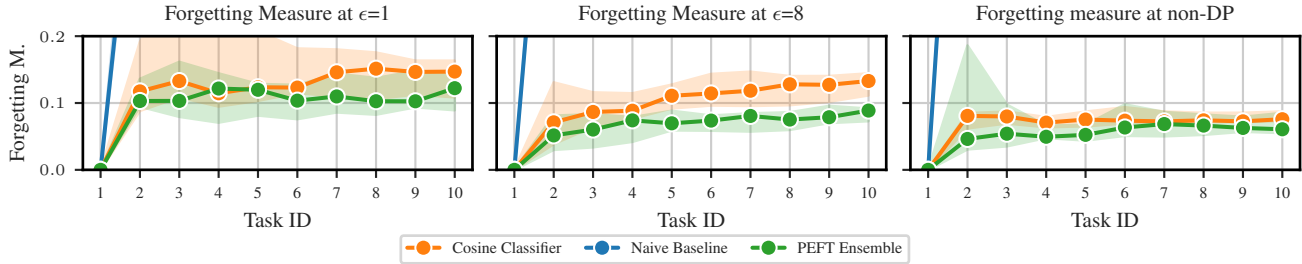


Figure A.5. Median forgetting measure per task on ImageNet-R (ViT-B pre-trained on ImageNet-21k). The error bars are the min/max forgetting measure obtained over five repeats with different class ordering, hyperparameter tuning runs and DP noise.

J.3. 5-dataset

In this section we analyse the results the results of 5-datasets. They are displayed in Figs. A.6 and A.7 and Table A5.

Table A5. Average accuracy (AA) and average forgetting (AF) (scaled by 100) after learning the final task in % on 5-dataset. We report the mean and std of the metrics averaged over all task order permutations.

Method	$\epsilon = 1, \delta = 1e-5$		$\epsilon = 8, \delta = 1e-5$		non-DP	
	AA (\uparrow)	AF (\downarrow)	AA (\uparrow)	AF (\downarrow)	AA (\uparrow)	AF (\downarrow)
Naive	15.93 \pm 1.35	85.00 \pm 5.00	17.56 \pm 1.35	90.00 \pm 2.00	13.15 \pm 5.84	79.00 \pm 12.00
Cosine classifier	58.54 \pm 0.35	1.00 \pm 0.00	59.78 \pm 0.07	0.00 \pm 0.00	59.87 \pm 0.00	0.00 \pm 0.00
PEFT Ensemble (FiLM)	79.69 \pm 3.51	5.00 \pm 4.00	87.83 \pm 0.00	3.00 \pm 2.00	65.75 \pm 15.07	14.00 \pm 11.00

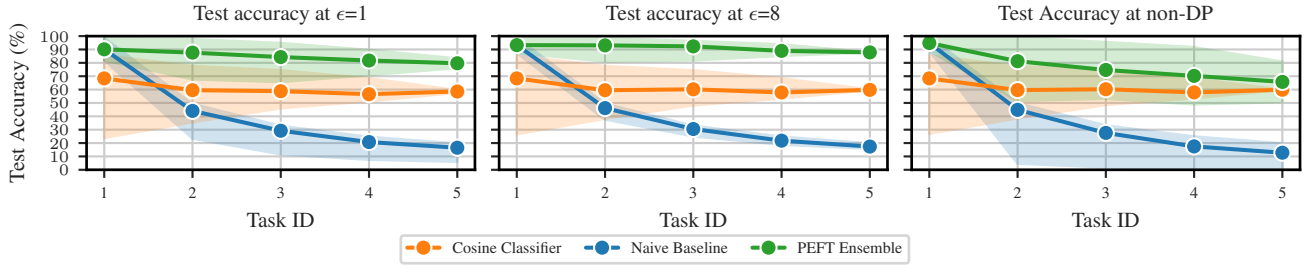


Figure A.6. Median test accuracy per task on 5-dataset (ViT-B pre-trained on ImageNet-21k). The error bars are the min/max test accuracy obtained over all permutations of tasks after training three models with hyperparameter tuning runs and DP noise.

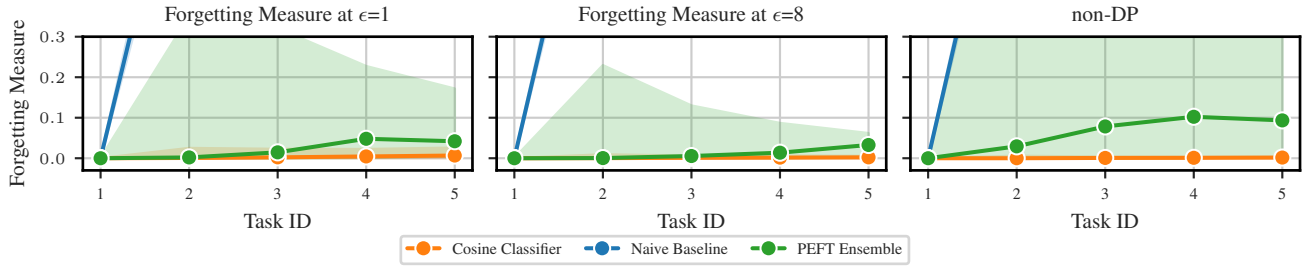


Figure A.7. Median forgetting measure per task on 5-dataset (ViT-B pre-trained on ImageNet-21k). The error bars are the min/max forgetting measure obtained over all permutations of tasks after training three models with hyperparameter tuning runs and DP noise.